NASA TM SX-732

NASA TM SX-732

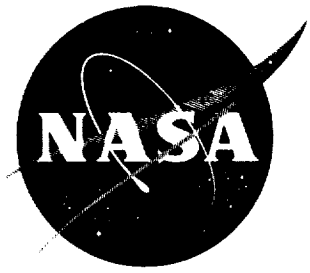

TECHNICAL MEMORANDUM

SX-732

for

Bureau of Naval Weapons, Department of the Navy

LONGITUDINAL AND LATERAL STABILITY AND CONTROL CHARACTERISTICS OF A 1/9-SCALE MODEL OF A TWIN-RAMJET CANARD TARGET DRONE AT MACH NUMBERS FROM 0.60 TO 2.80

By M. Leroy Spearman

Langley Research Center
Langley Station, Hampton, Va.

NATIONAL AERONAUTICS AND SPACE ADMINISTRATION

WASHINGTON

AUG 14 1962

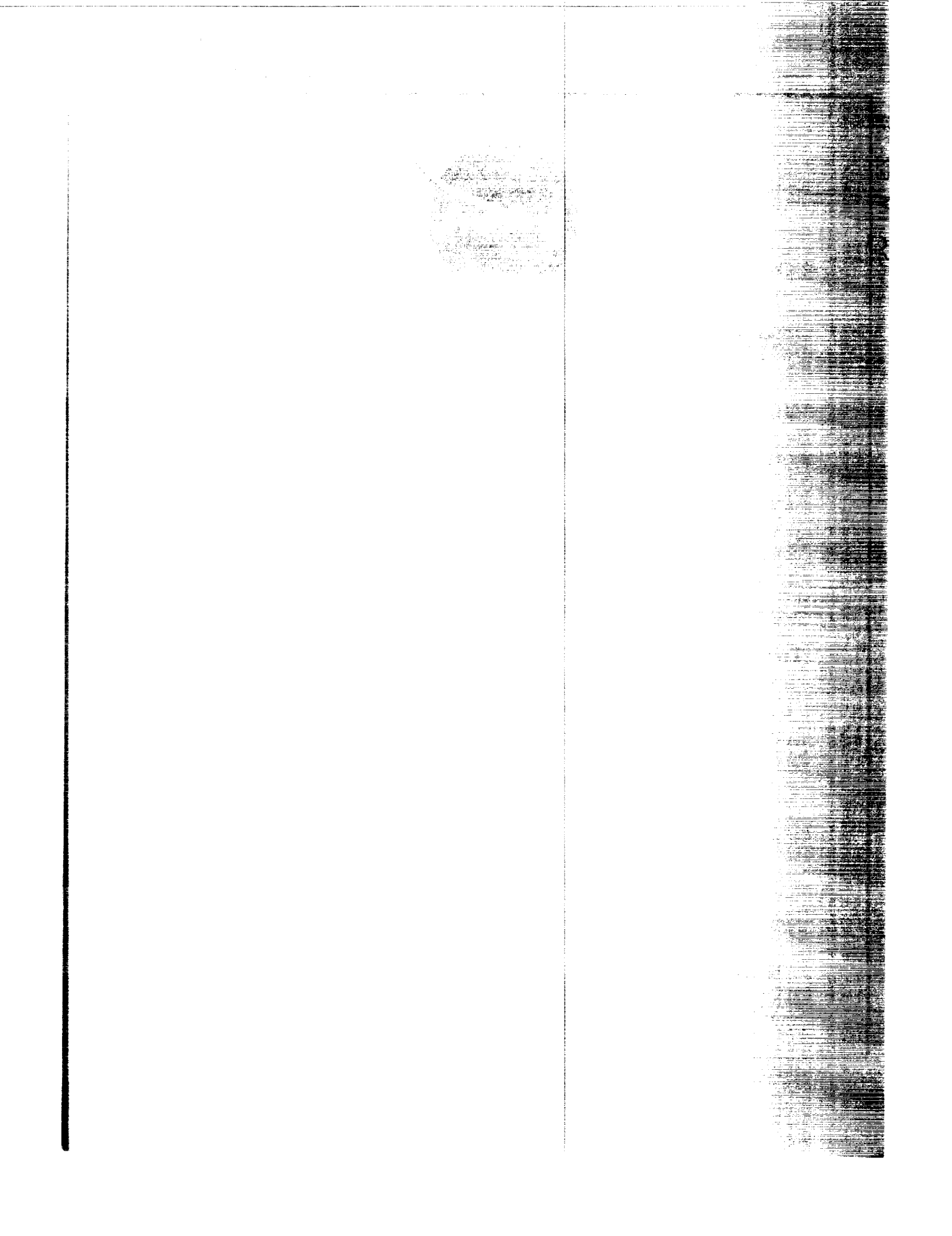

NATIONAL AERONAUTICS AND SPACE ADMINISTRATION

TECHNICAL MEMORANDUM SX-732

for

Bureau of Naval Weapons, Department of the Navy

LONGITUDINAL AND LATERAL STABILITY AND CONTROL CHARACTERISTICS OF A 1/9-SCALE MODEL OF A TWIN-RAMJET CANARD TARGET DRONE AT MACH NUMBERS FROM 0.60 TO 2.80

By M. Leroy Spearman

ABSTRACT

Tests were made in the Langley 8-foot transonic pressure tunnel at Mach numbers from 0.60 to 1.20 and in the Langley Unitary Plan tunnel at Mach numbers of 1.60, 1.80, 2.16, and 2.80. Tests were made at combined angles of attack and sideslip with various combinations of control deflections for the model both with and without boosters.

NATIONAL AERONAUTICS AND SPACE ADMINISTRATION

TECHNICAL MEMORANDUM SX-732

for

Bureau of Naval Weapons, Department of the Navy

LONGITUDINAL AND LATERAL STABILITY AND CONTROL CHARACTERISTICS OF A 1/9-SCALE MODEL OF A TWIN-RAMJET CANARD TARGET DRONE AT MACH NUMBERS FROM 0.60 TO 2.80

By M. Leroy Spearman

SUMMARY

An investigation has been conducted at the Langley Research Center to determine the stability and control characteristics of a 1/9-scale model of a twin-ramjet canard target drone at Mach numbers from 0.60 to 2.80. The drone was tested both with and without twin boosters. The results indicate that some stability and trim problems may occur as a result of booster separation, interference effects of the canard flow field, and low lateral-control effectiveness.

INTRODUCTION

An investigation has been conducted at the Langley Research Center to determine the stability and control characteristics of a 1/9-scale model of a target drone at Mach numbers from 0.60 to 2.80. The drone is a canard configuration powered by twin ramjet engines pylon-mounted in the horizontal plane and it is designed to cruise in the Mach number range from 2.0 to 2.5. The drone is boosted to a Mach number of about 1.6 by twin boosters attached to the forward part of the body. Pitch control is provided by a canard surface and lateral control is provided by an off-on type of spoiler attached to the trailing edge of a small surface mounted outboard of the nacelles. No provision is made for yaw control.

The purpose of the investigation was to determine if there were any major problem areas with the configuration and to provide aerodynamic parameters that could be used in simulator studies. The results are presented with only a limited analysis.

SYMBOLS

The results are referred to the body-axis system with the moment center located on the body center line at a point 56.1 percent of the body length.

The symbols are defined as follows:

C_l	rolling-moment coefficient, $\frac{\text{Rolling moment}}{qSl}$
C_m	pitching-moment coefficient, $\frac{\text{Pitching moment}}{qSc}$
$C_{m,o}$	pitching-moment coefficient at $C_N = 0$
C_N	normal-force coefficient, $\frac{\text{Normal force}}{qS}$
C_n	yawing-moment coefficient, $\frac{\text{Yawing moment}}{qSl}$
c	reference chord, 0.627 ft
l	reference length, 0.627 ft
M	Mach number
q	free-stream dynamic pressure, lb/sq ft
S	reference area, 0.4106 sq ft
α	angle of attack, deg
β	angle of sideslip, deg
δ_c	deflection of canard surface, deg
δ_s	spoiler deflection, deg
$\frac{\partial C_m}{\partial C_N}$	longitudinal-stability parameter

MODEL AND APPARATUS

Details of the model are shown in figure 1. Photographs showing the model both with and without the boosters are presented in figure 2. The fuselage was basically circular in cross section except for a region near the nose which was flattened to permit deflection of the canard surface without unporting. The canard surface could be manually adjusted in increments of 5° for a deflection range from -10° to 10°. The spoiler control consisted of small surfaces located outboard of the nacelles from which a trailing-edge mounted plate could be projected vertically. The spoiler could be set for either an off position or for a fully projected position. Various antennas and control housings were simulated

n the model. The model was sting mounted on a six-component internal strain-gage alance. Sample schlieren photographs of the model (fig. 3) show two different nlet arrangements for which internal-flow measurements were obtained simultaneusly. All force data presented herein are for the shorter nacelle arrangement.

TEST CONDITIONS

Transonic tests were made in the Langley 8-foot transonic pressure tunnel rom $M = 0.60$ to $M = 1.20$ for the drone with boosters and from $M = 0.75$ to $= 1.20$ for the drone without boosters. Supersonic tests were made in the angley Unitary Plan tunnel at $M = 1.60$ and 1.80 for the model with boosters nd at $M = 1.60$, 2.16, and 2.80 for the drone without boosters. The Reynolds umber per foot varied from about 1.6×10^6 at $M = 0.60$ to 2.1×10^6 at $= 1.20$ and from about 2.25×10^6 at $M = 1.60$ to 2.45×10^6 at $M = 2.80$. n order to provide a turbulent boundary layer, transition strips of carborundum articles were applied near the nose of the body, the boosters, and nacelles, and ear the leading edges of the canard surface, vertical tail, pylon struts, and poiler surfaces.

PRESENTATION OF RESULTS

The results of the investigation are presented in the following figures:

DISCUSSION

The basic longitudinal aerodynamic characteristics (figs. 4 and 5) indicate some erratic nonlinearities both in stability level and control effectiveness at subsonic speeds that generally tend to disappear at supersonic speeds. The longitudinal stability characteristics are summarized in figure 6 wherein the result from figures 4 and 5 have been transferred to center-of-gravity locations corresponding to those expected under flight conditions. These locations are at stations 20.3 for the model with the boosters and 24.8 for the model without the boosters. Large variations in $\partial C_m/\partial C_N$ and $C_{m,o}$ with Mach number are indicate for the configuration with the boosters. In addition, at the separation Mach number of 1.6 a substantial change in stability level is indicated that might induce dynamic stability problems.

The variation of C_n with α at a constant angle of sideslip for the configuration with the boosters (fig. 9) indicates a rapid decrease in directional stability with either a positive or a negative increase in angle of attack for all Mach numbers investigated. Without the boosters (fig. 11), the variation of C_n with α improves to the extent that at the higher Mach numbers the directional stability increases with increasing angle of attack as a result of an increase in the effectiveness of the lower vertical tail. In some cases, deflection of the canard surface had an adverse effect on the directional stability. In particular for the drone without boosters at high angles of attack for $M = 1.20$ and 1.60 (figs. 11 and 15), deflection of the canard surface causes a substantial reduction in directional stability as a result of the impingement of the flow field from the canard on the vertical tail. This flow field is shown in the schlieren photograph of figure 3.

The variation of C_l with α at a constant angle of sideslip for the missile both with and without the boosters (figs. 10 and 12) indicates a generally progressive increase in positive effective dihedral with increasing positive α and an increase in negative effective dihedral with increasing negative α. Deflection of the canard surface has a measurable effect on the lateral stability in that positive deflections generally increase the effective dihedral and negative deflections generally decrease the effective dihedral.

The effectiveness of the spoiler in producing C_l through the angle-of-attack range is shown in figures 17 and 18 for the missile with and without the boosters. These data have been used in conjunction with the effective-dihedral results to

letermine the angles of sideslip for which the rolling moment can be trimmed to zero. (See fig. 19.) As the angle of attack is increased, the angles of sideslip for which the rolling moments can be trimmed become very small in some cases. Although flight under conditions of sideslip may not be anticipated, such conditions might occur as a result of asymmetric thrust or of dynamic oscillations that might be induced by booster separation.

CONCLUDING REMARKS

An investigation has been conducted at the Langley Research Center to determine the stability and control characteristics of a 1/9-scale model of a twin-ramjet canard target drone at Mach numbers from 0.60 to 2.80. The drone was tested both with and without twin boosters. The results indicated that some stability and trim problems may occur as a result of booster separation, interference effects of the canard flow field, and low lateral-control effectiveness.

Langley Research Center,
National Aeronautics and Space Administration,
Langley Station, Hampton, Va., July 18, 1962.

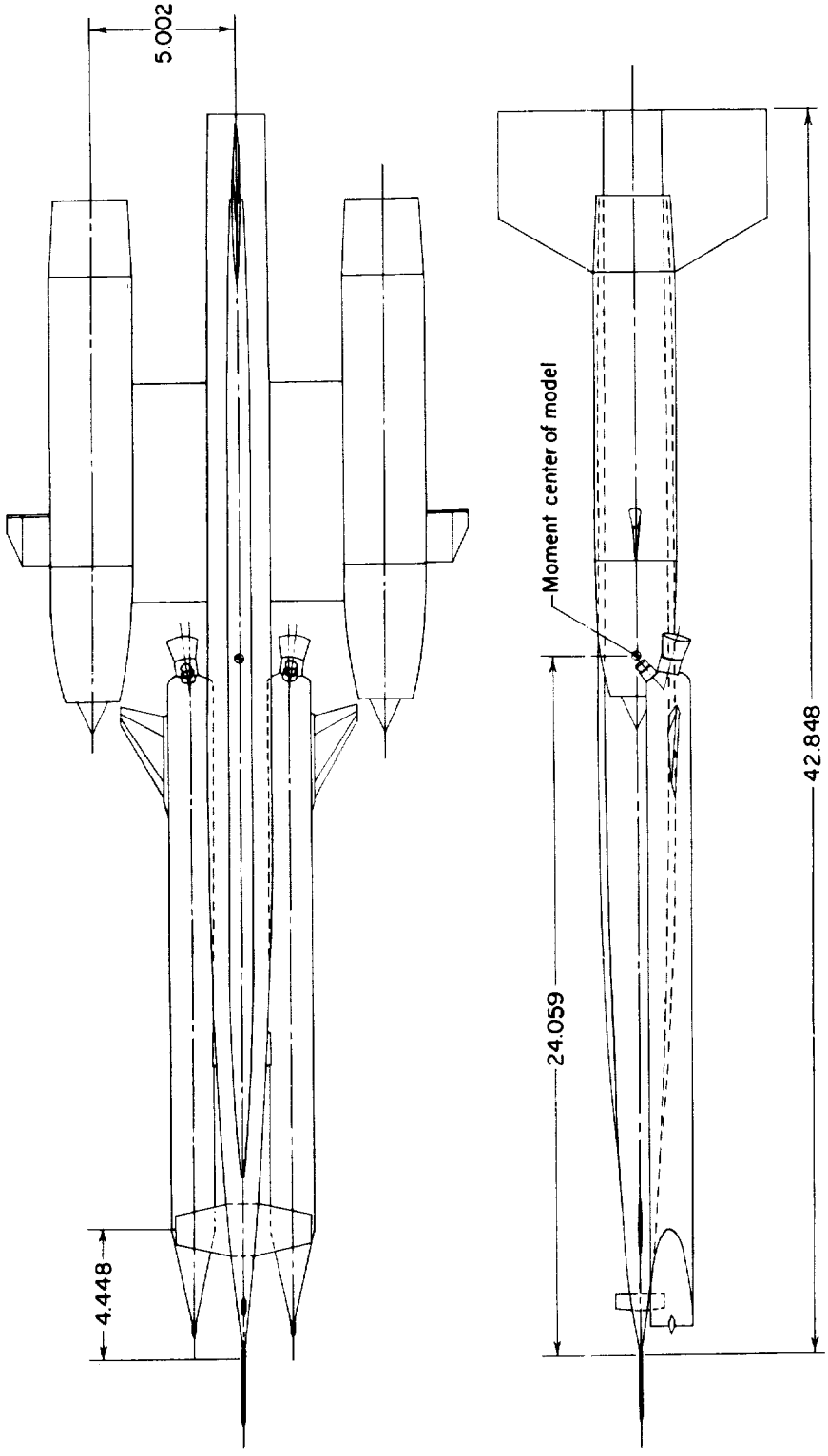

Figure 1.- Details of model. All dimensions are in inches.

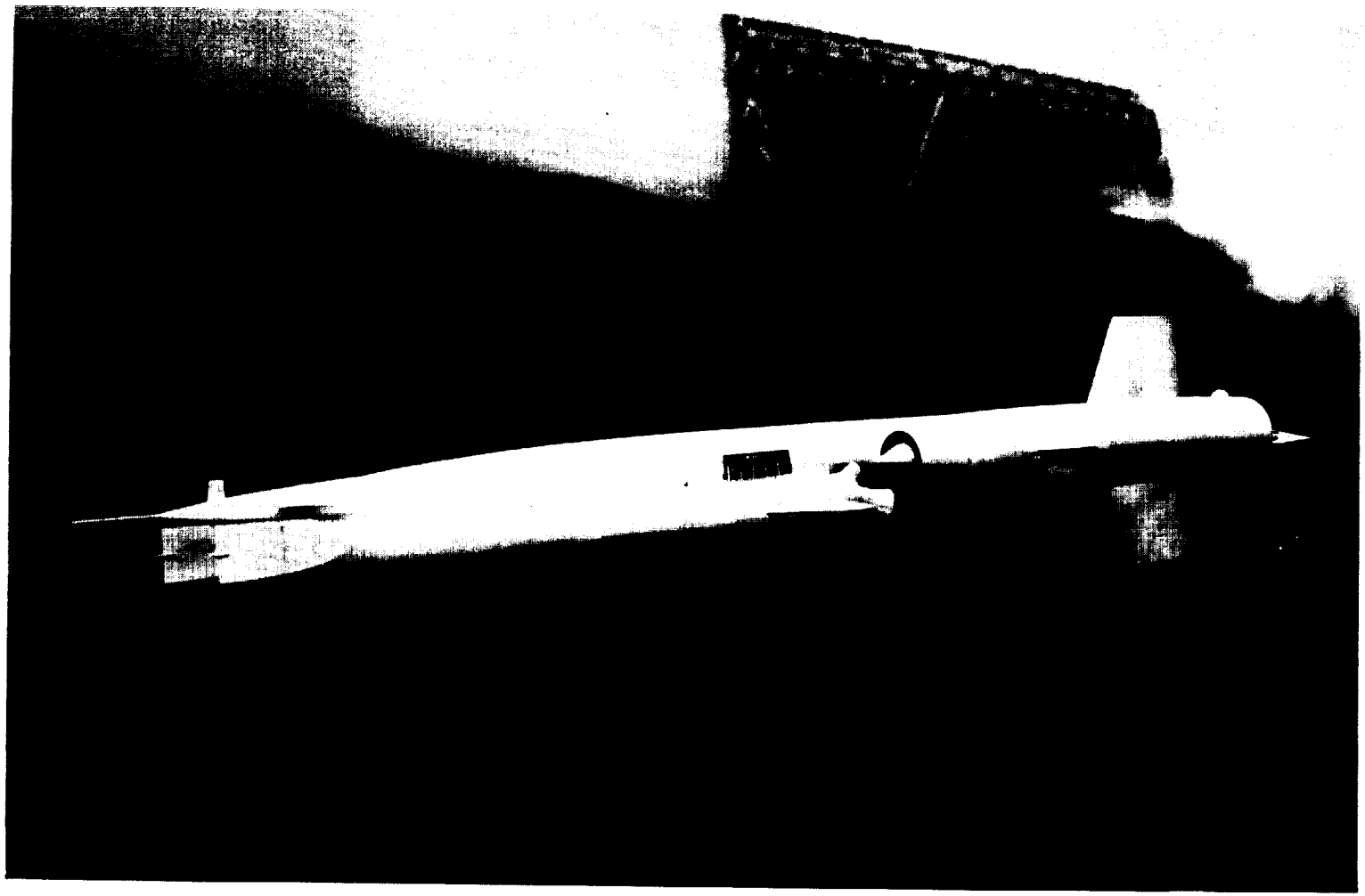

(a) Drone with boosters. L-61-8691

Figure 2.- Photographs of model.

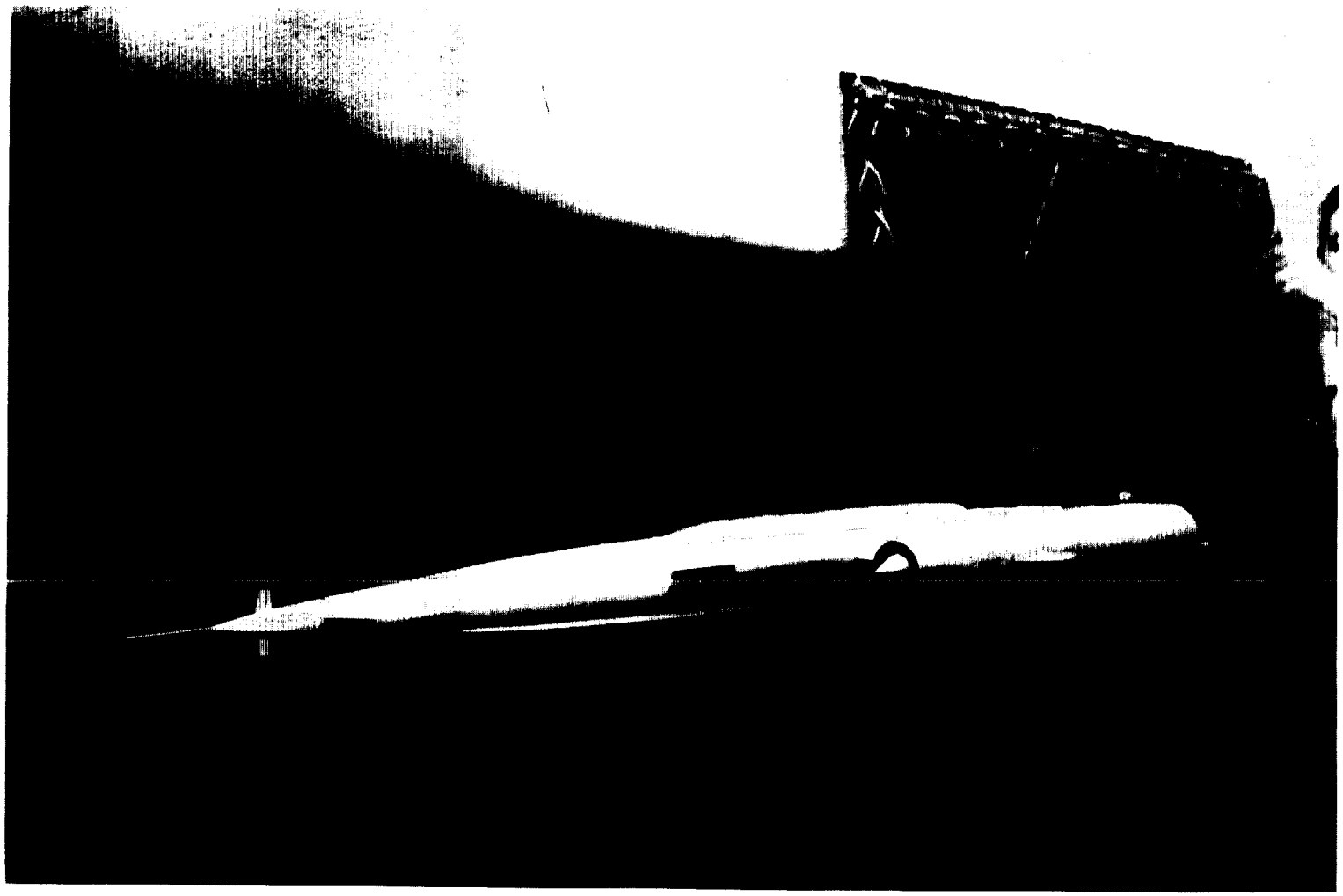

(b) Drone without boosters. L-61-8690

Figure 2.- Concluded.

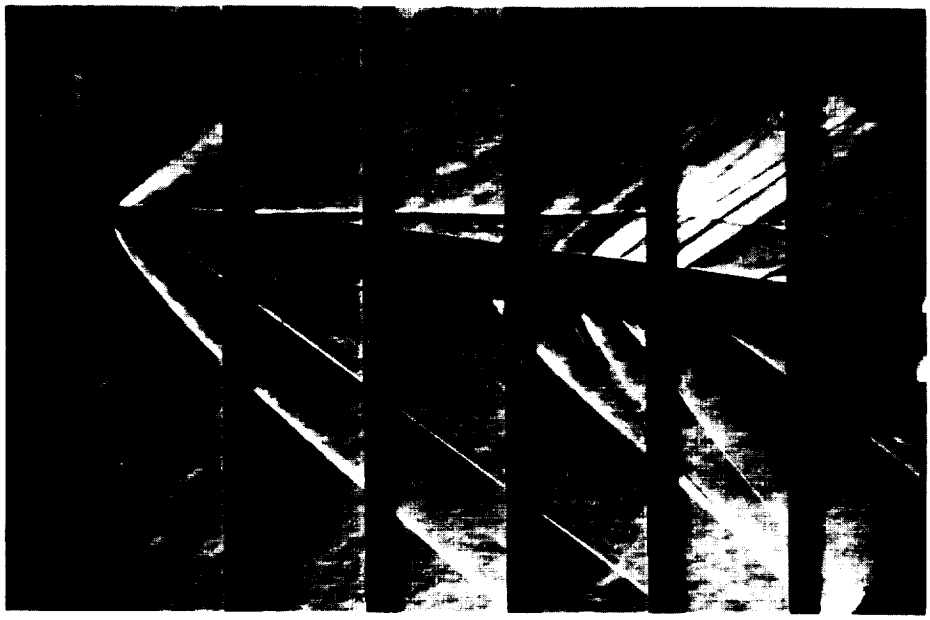

(a) Side view. $\alpha \approx 11^{\circ}$; $\beta = 0^{\circ}$.

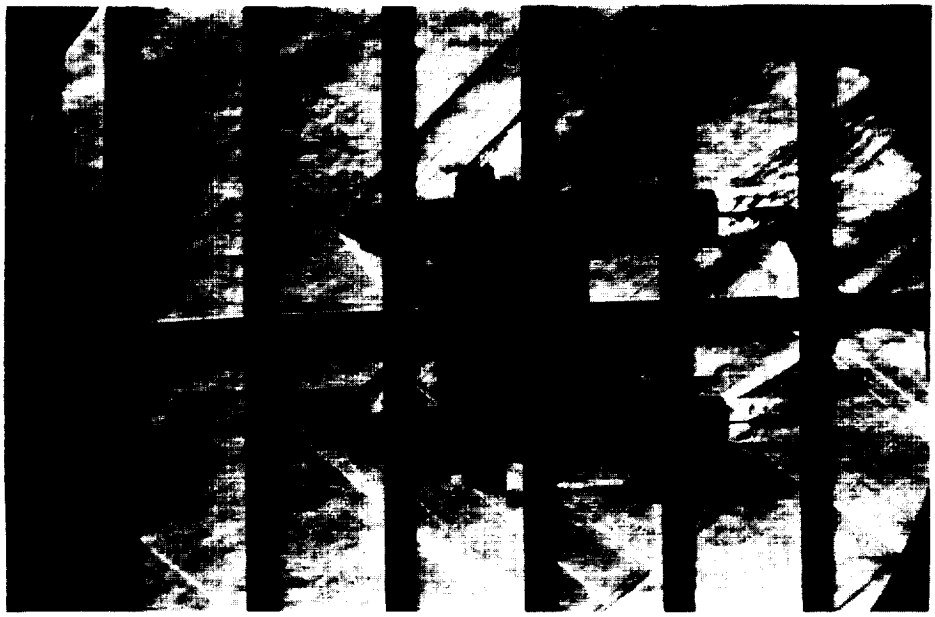

(b) Top view. $\alpha \approx 0^{\circ}$; $\beta = 2^{\circ}$. L-62-2111

Figure 3.- Schlieren photographs of drone without boosters. $M = 1.60$; $\delta_c = 10^{\circ}$.

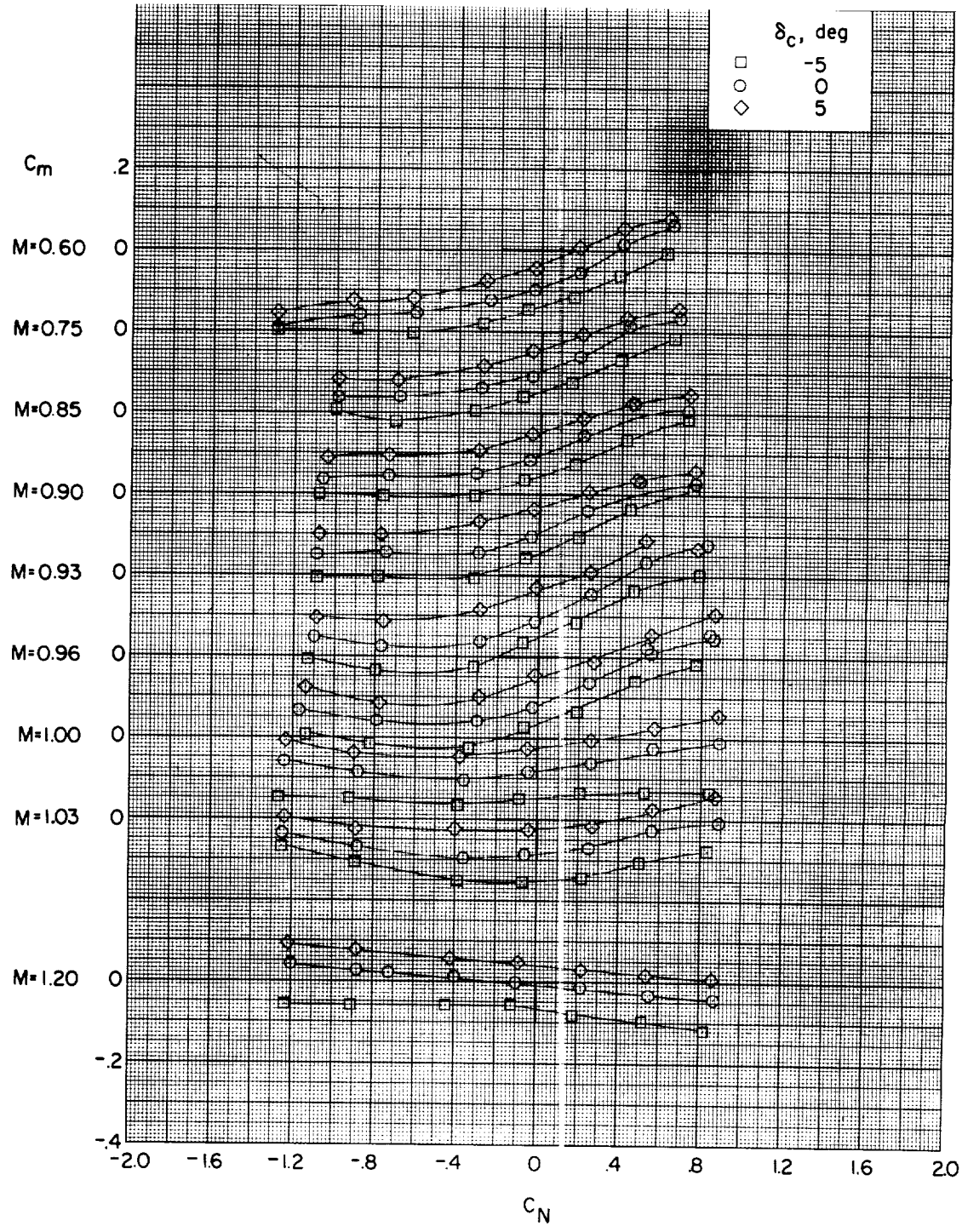

Figure 4.- Effect of canard deflection on variation of C_m with C_N (drone with boosters). $\beta = 0^\circ$.

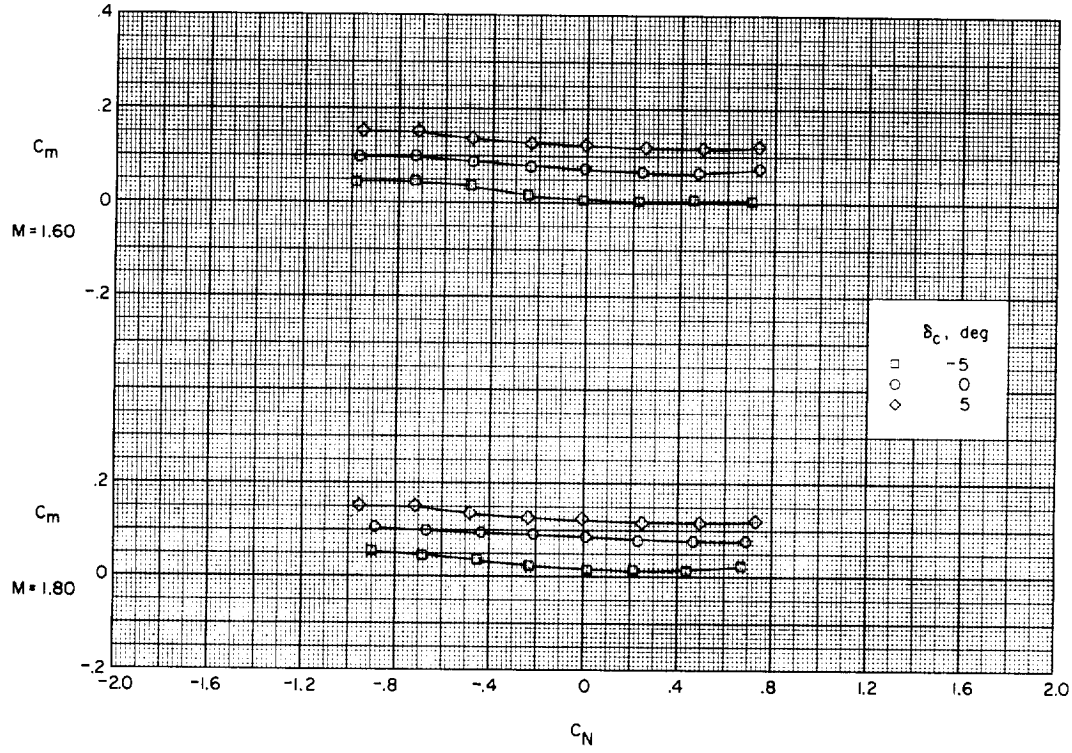

Figure 4.- Concluded.

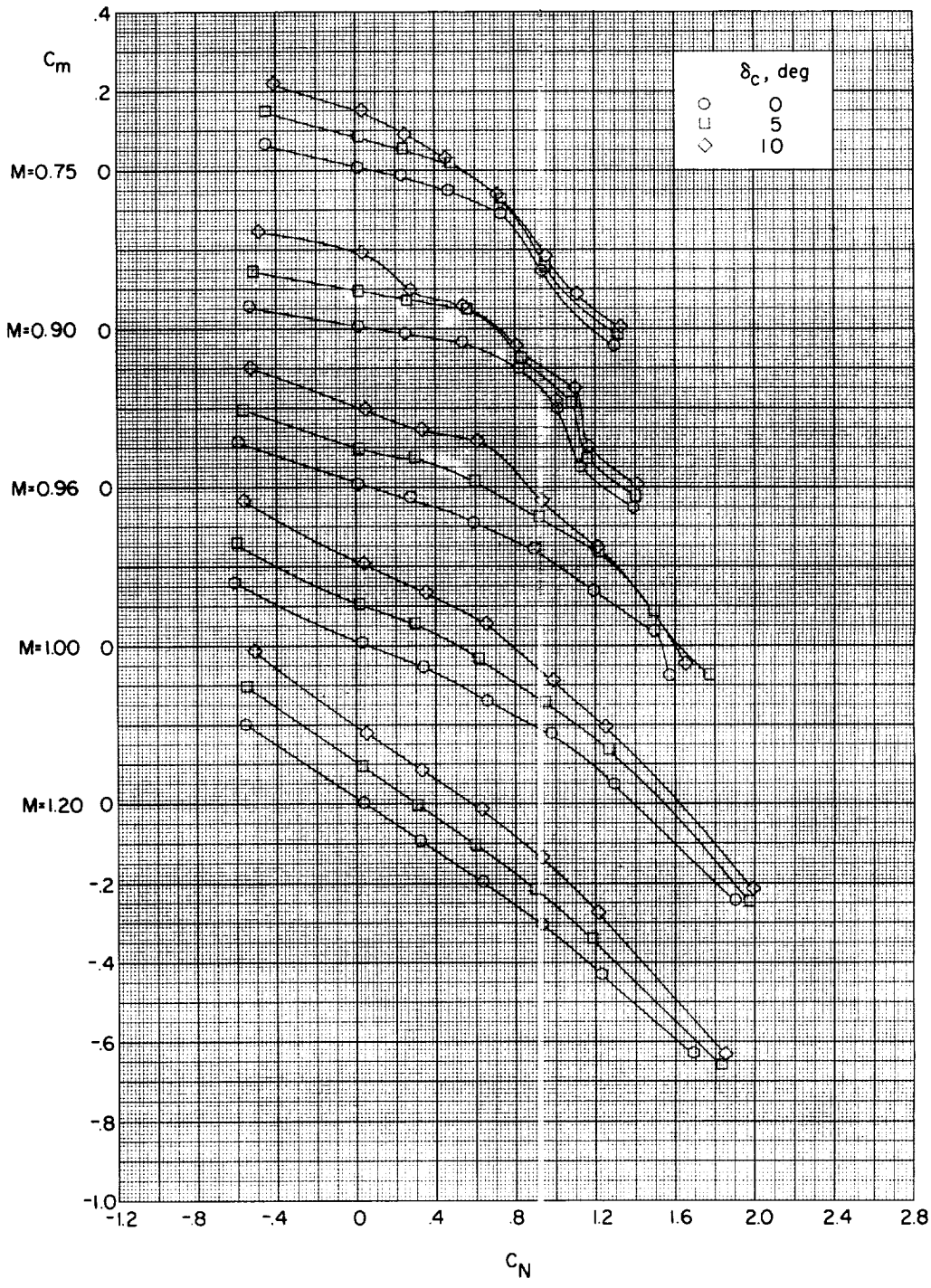

Figure 5.- Effect of canard deflection on variation of C_m with C_N (drone without boosters). $\beta = 0^\circ$.

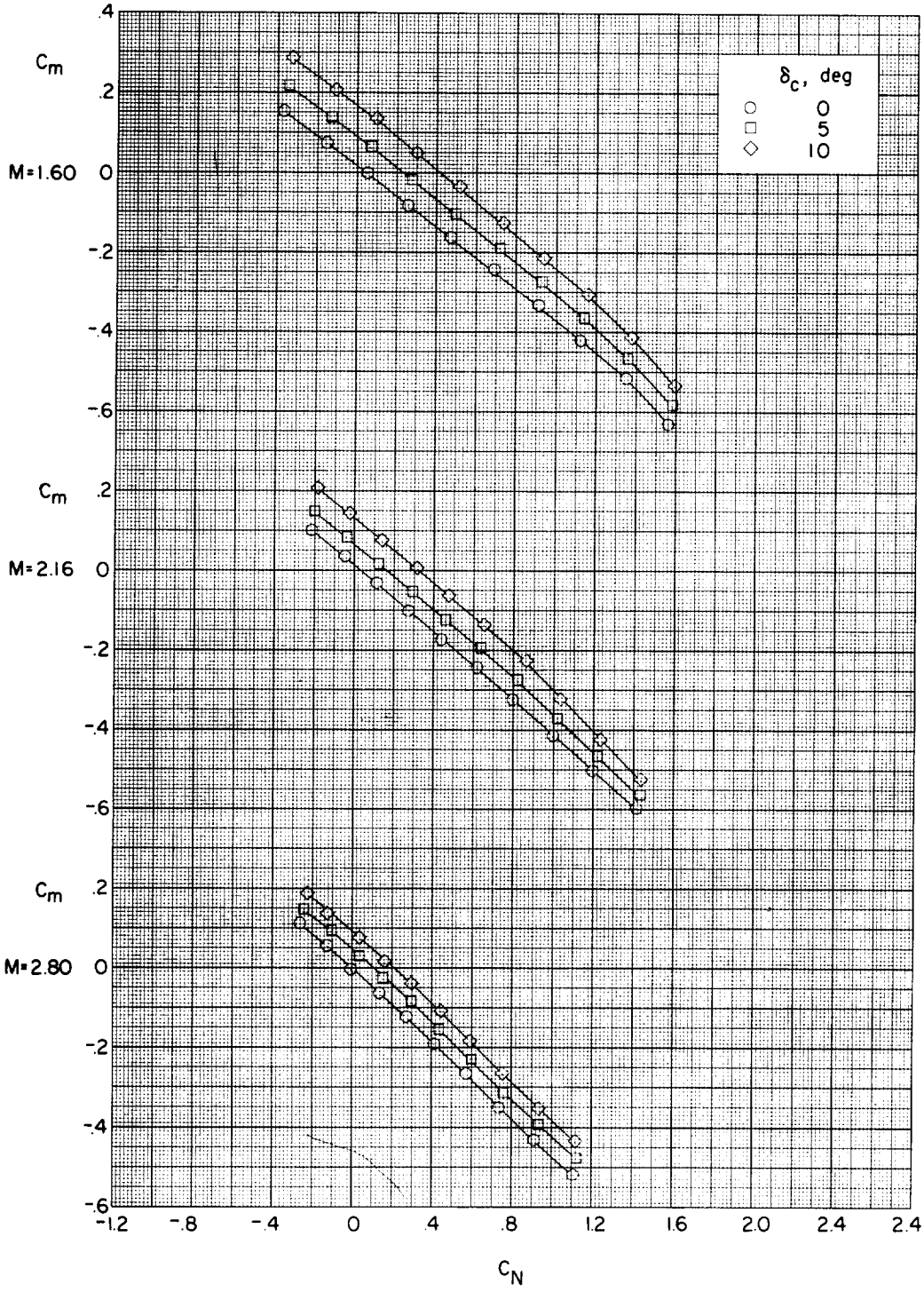

Figure 5.- Concluded.

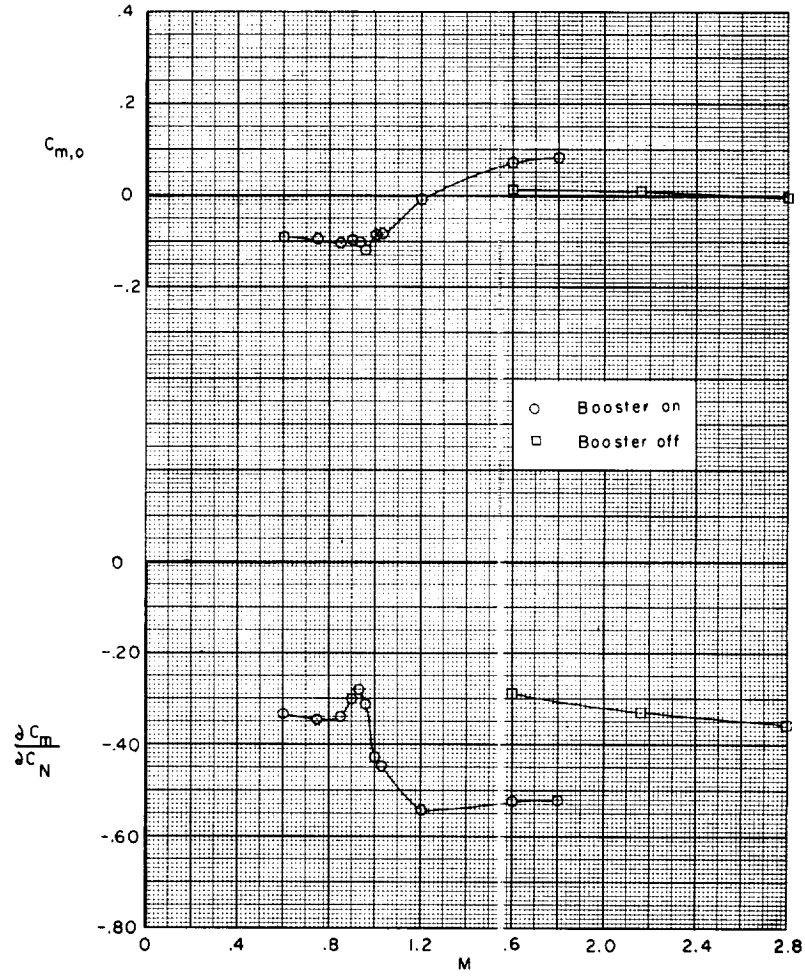

Figure 6.- Summary of longitudinal stability characteristics of model.

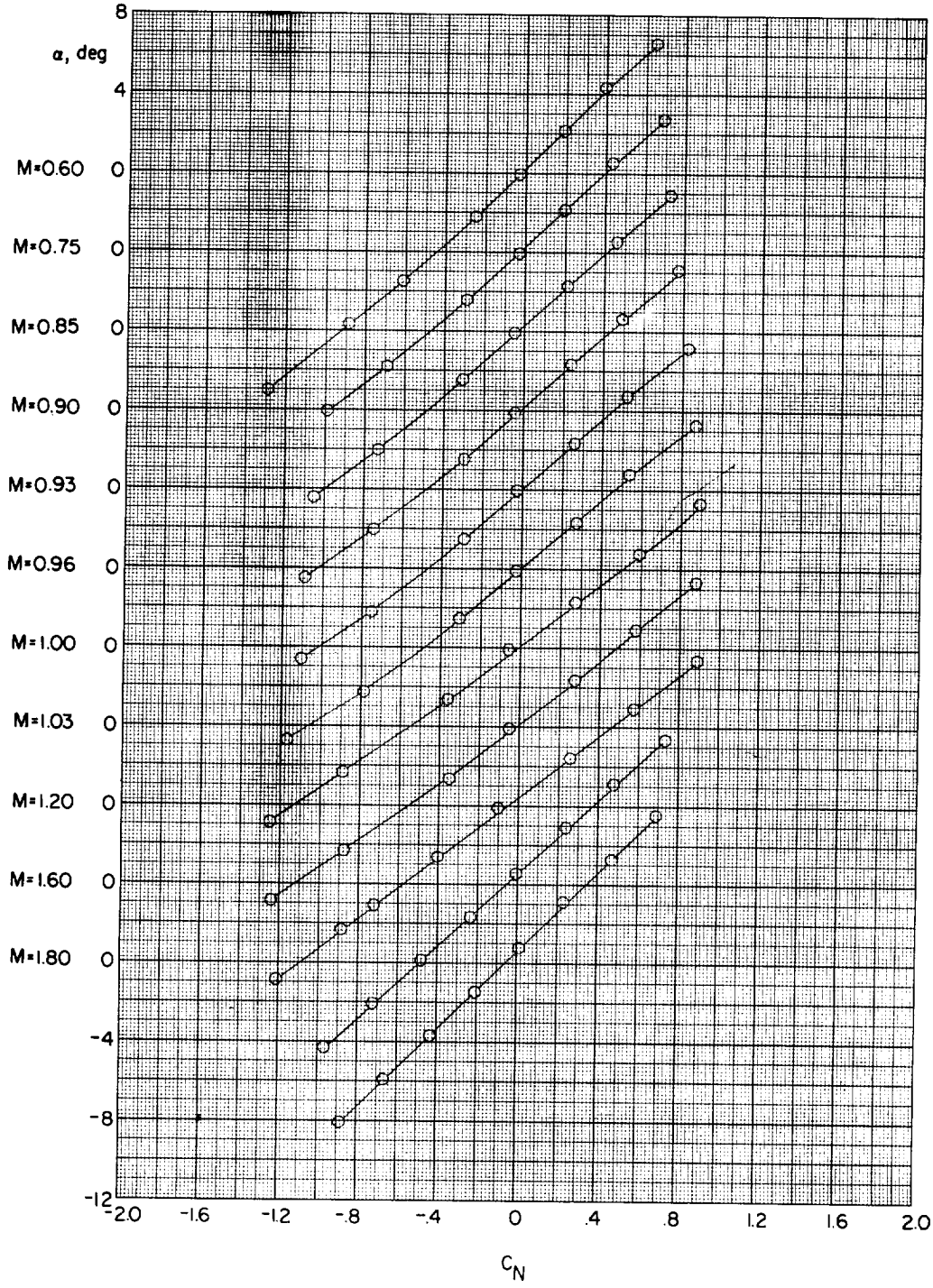

Figure 7.- Variation of α with C_N for drone with boosters. $\beta = 0^o$; $\delta_c = 0^o$.

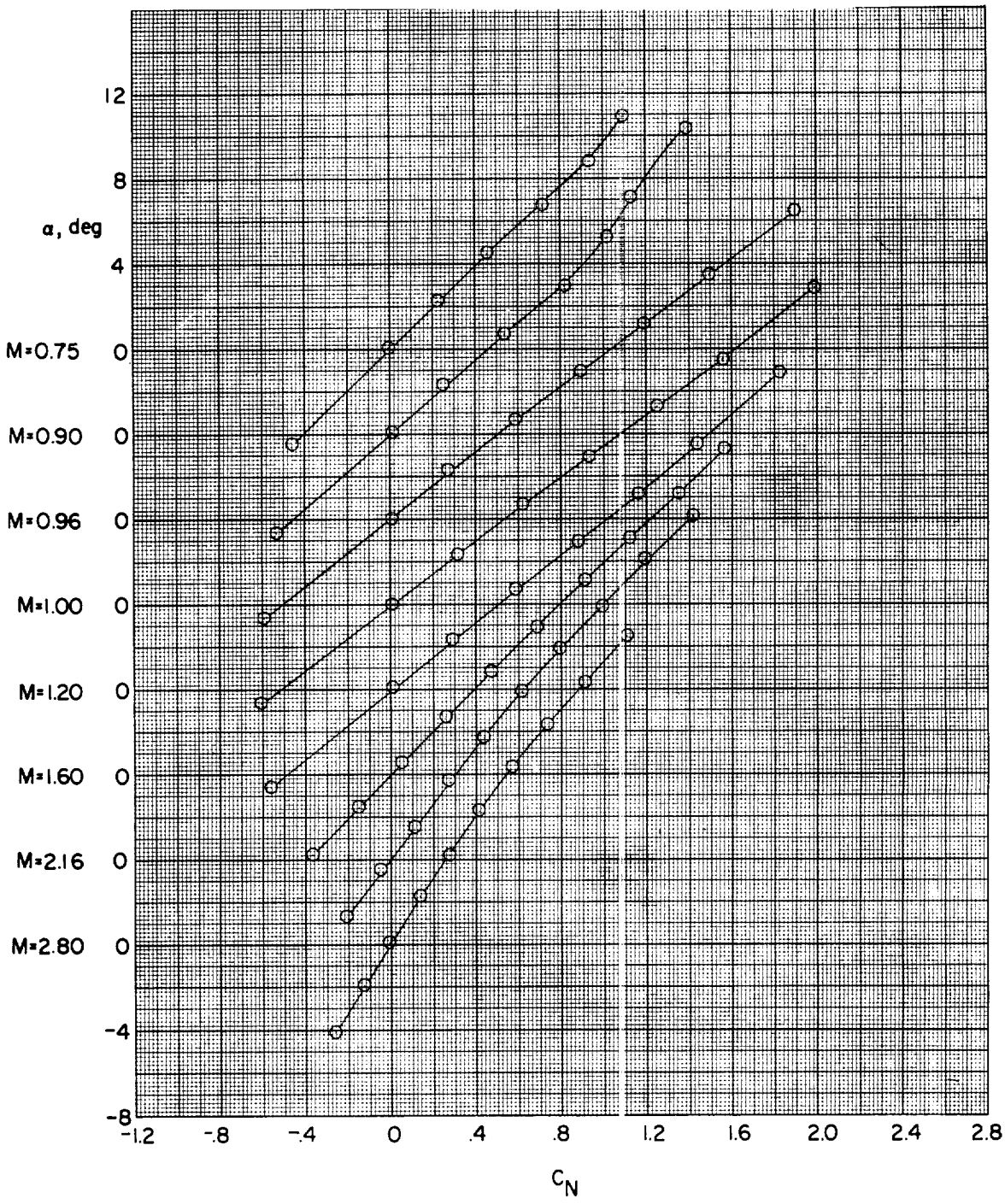

Figure 8.- Variation of α with C_N for drone without boosters. $\beta = 0^\circ$; $\delta_c = 0^\circ$.

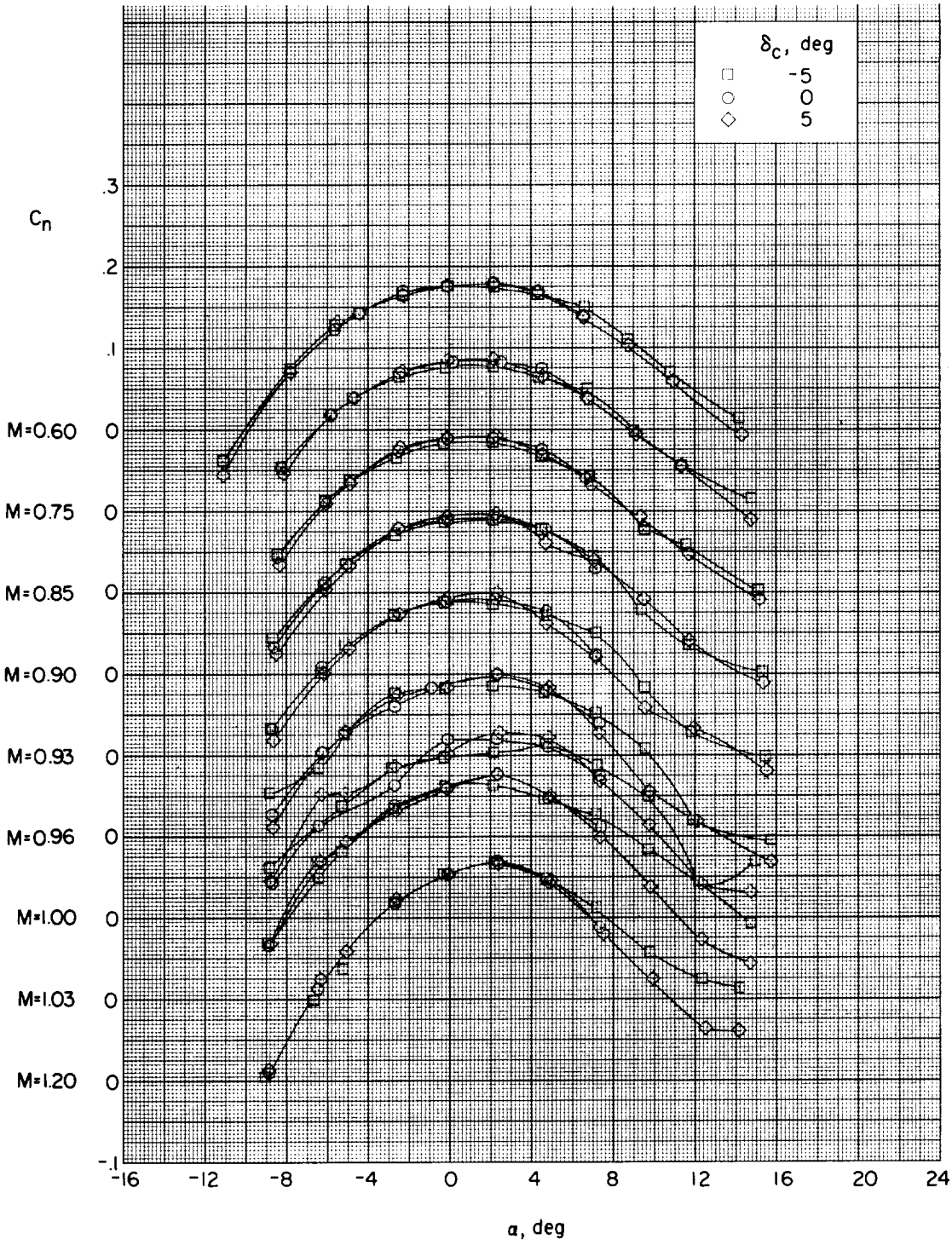

Figure 9.- Effect of canard deflection on variation of C_n with α (drone with boosters). $\beta \approx 5.1^{\circ}$.

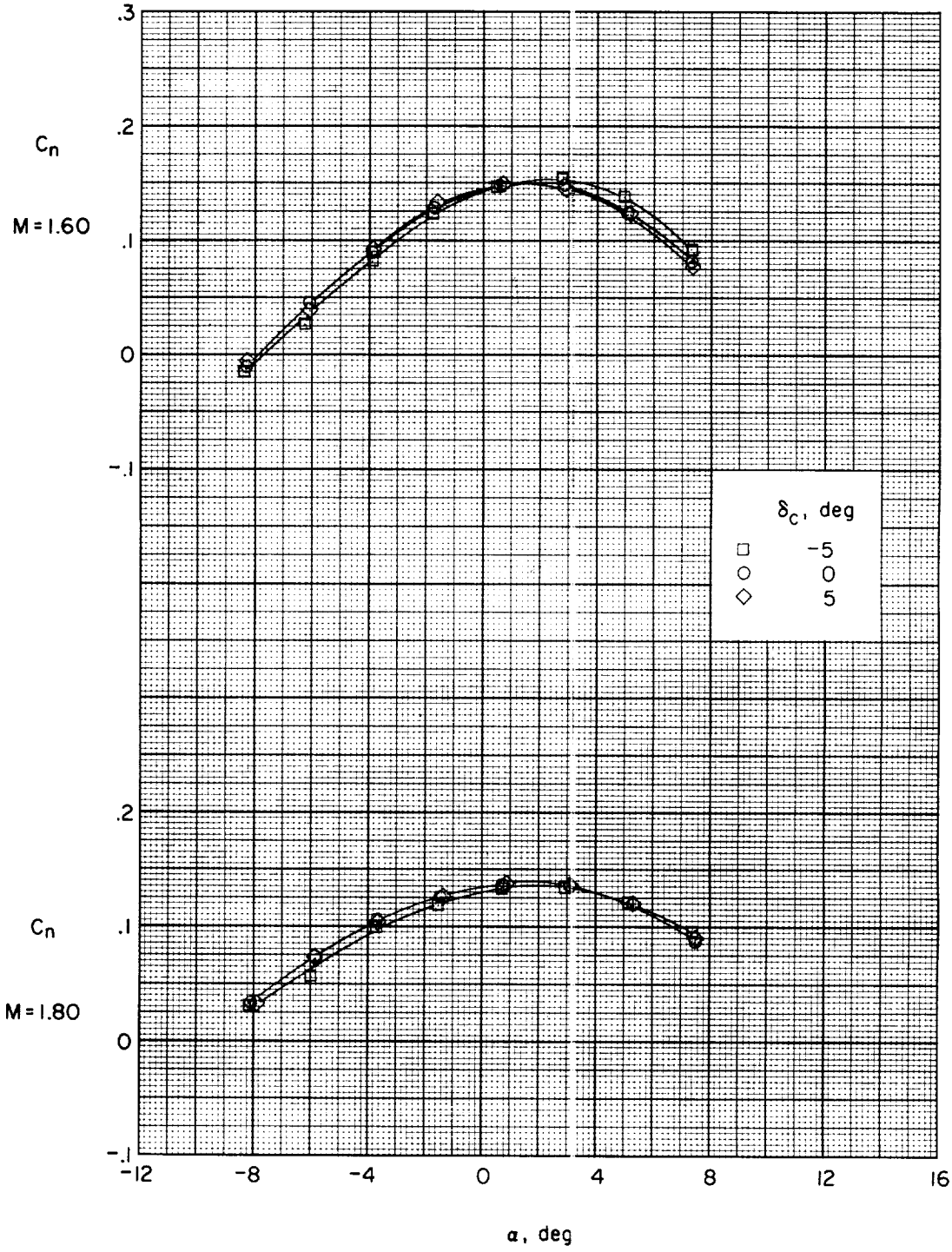

Figure 9.- Concluded.

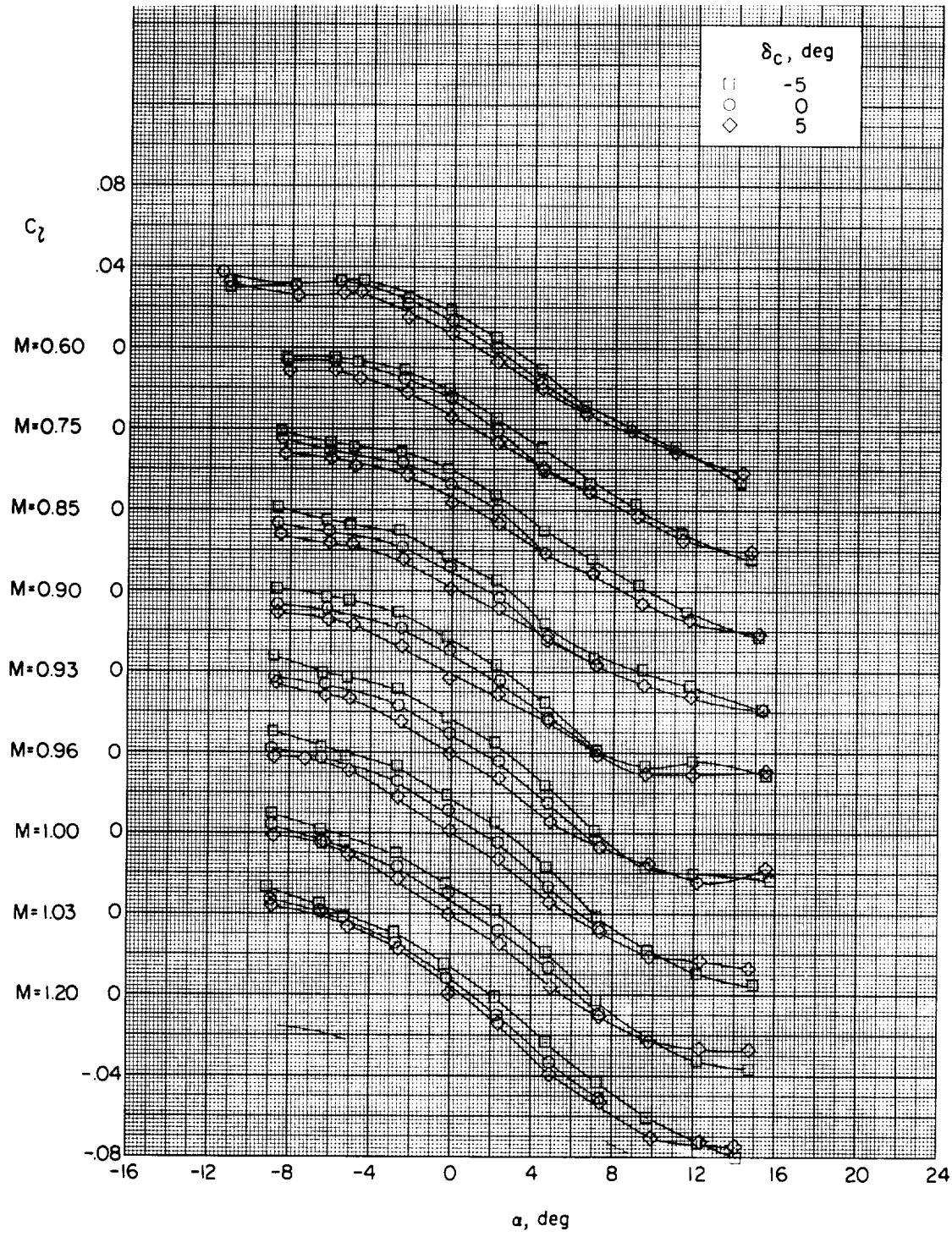

Figure 10.- Effect of canard deflection on variation of C_l with α (drone with boosters). $\beta \approx 5.1^{\circ}$.

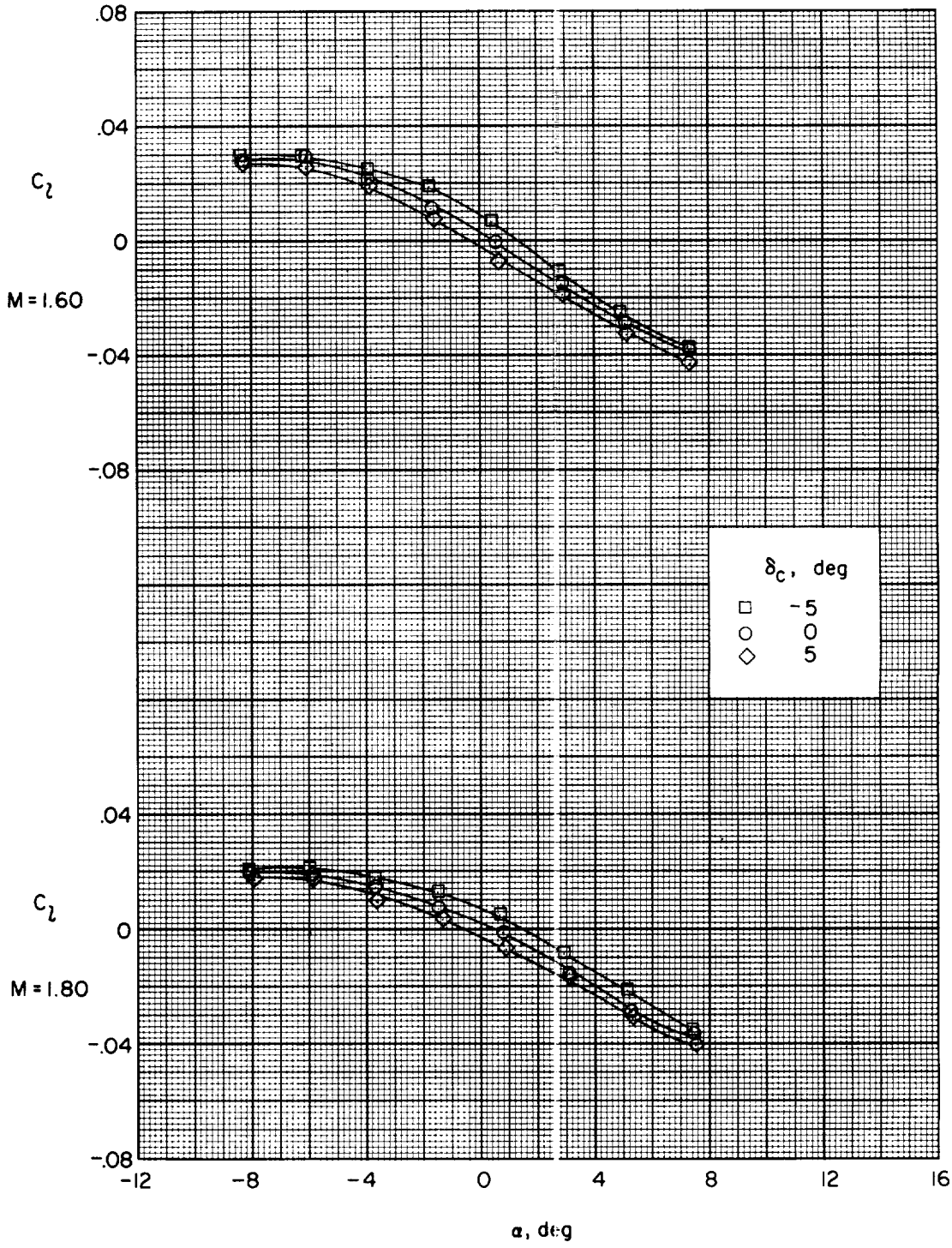

Figure 10.- Concluded.

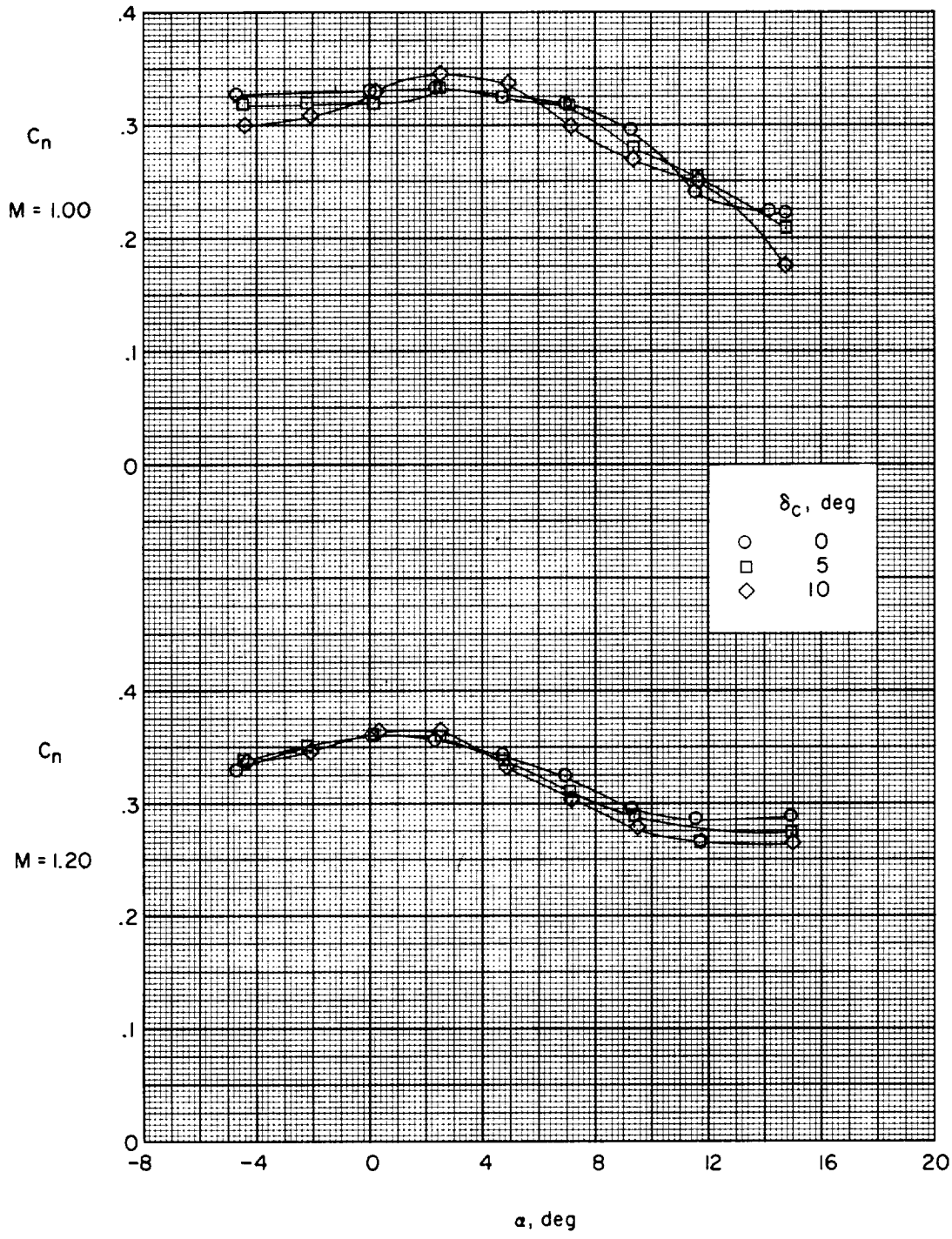

Figure 11.- Effect of canard deflection on variation of C_n with α (drone without boosters). $\beta \approx 5^\circ$.

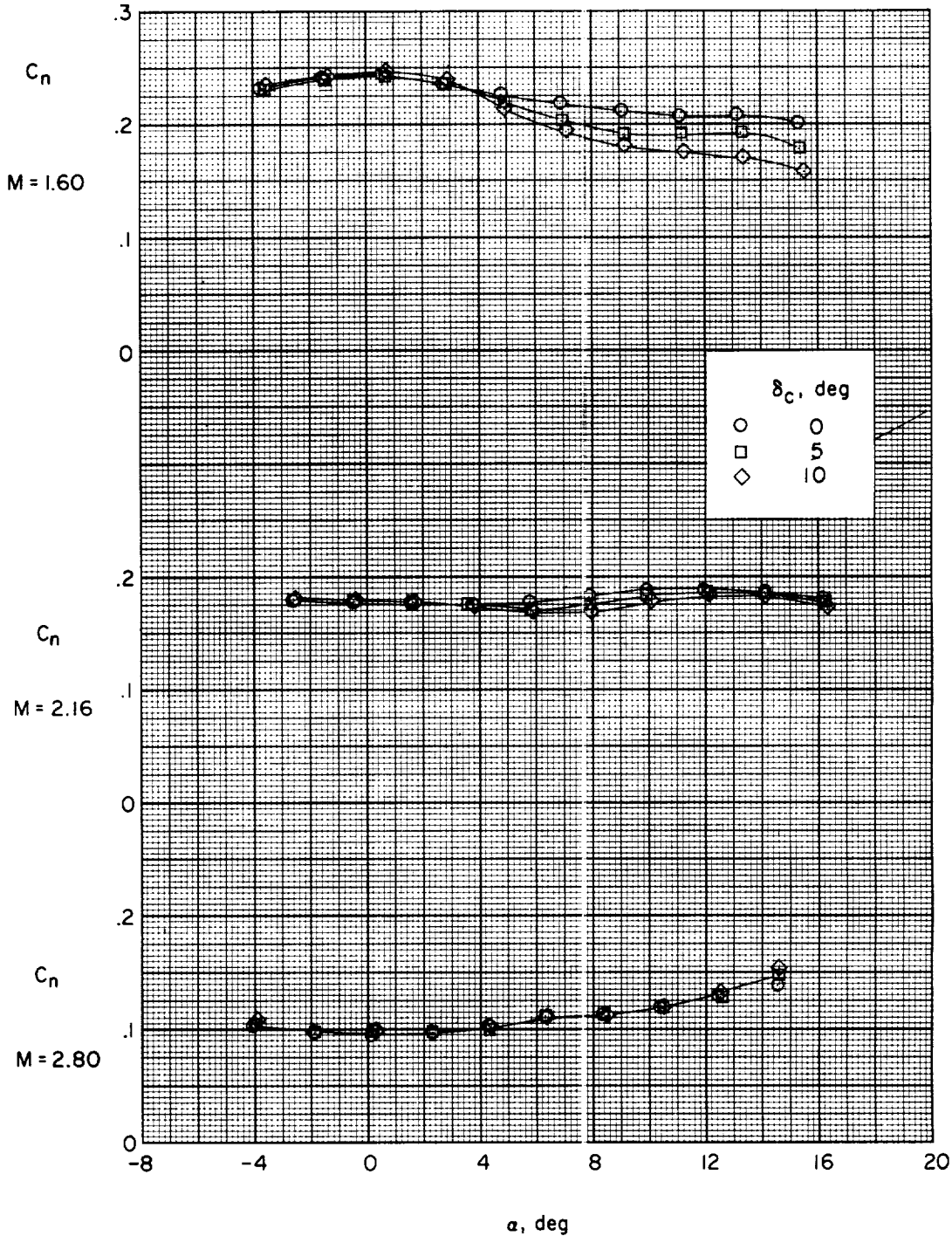

Figure 11.- Concluded.

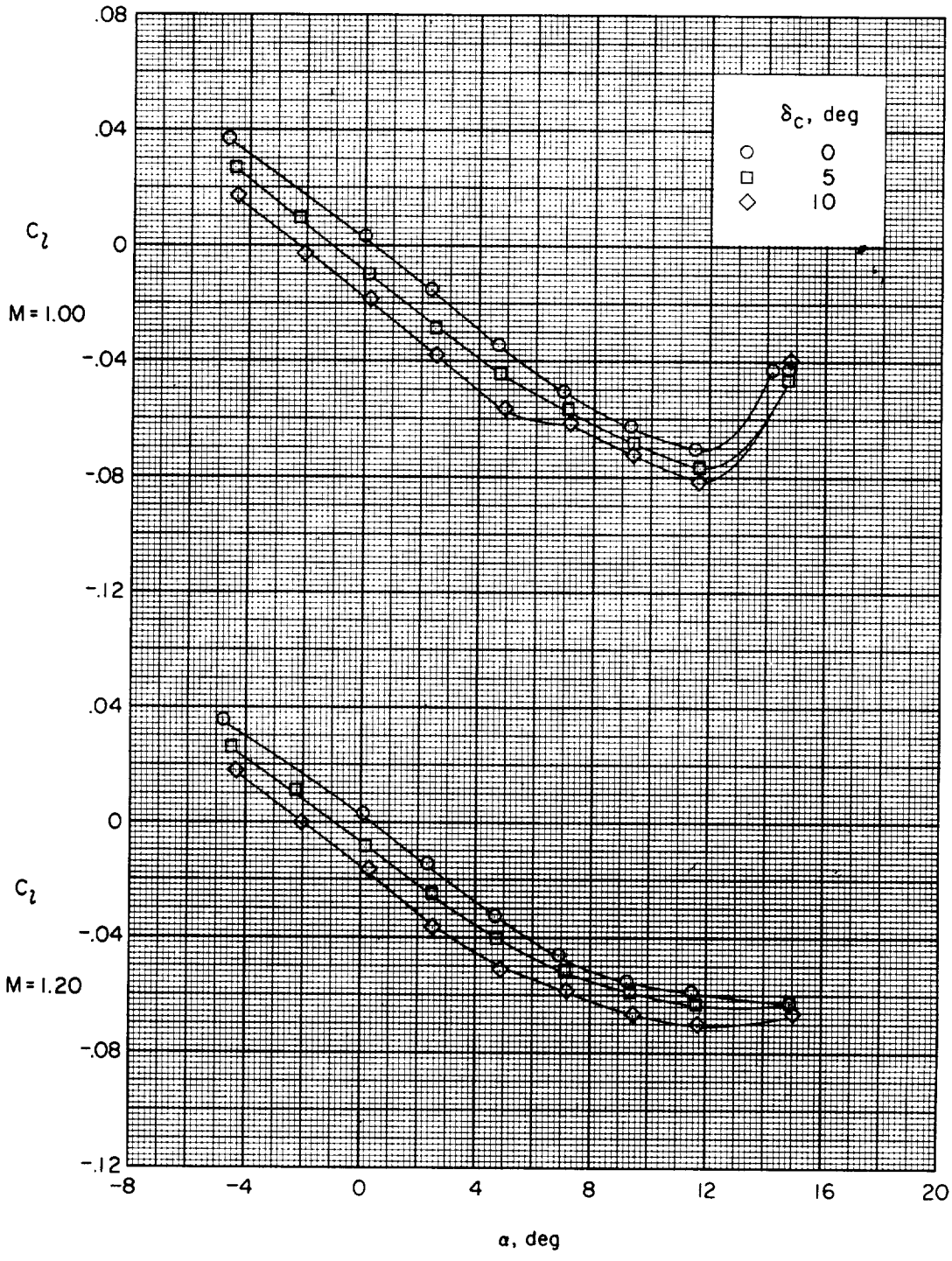

Figure 12.- Effect of canard deflection on variation of C_l with α (drone without boosters). $\beta \approx 5^\circ$.

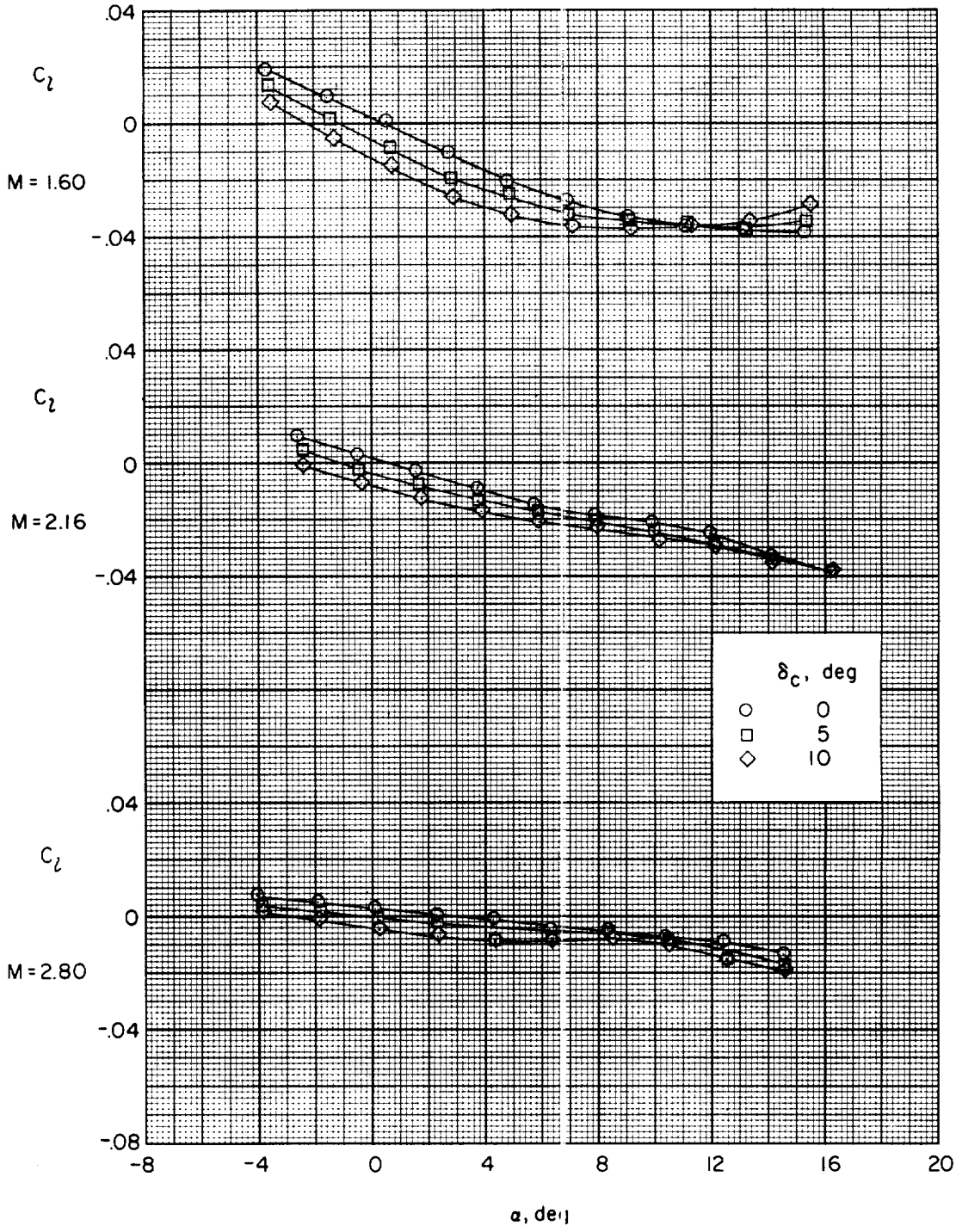

Figure 12.- Concluded.

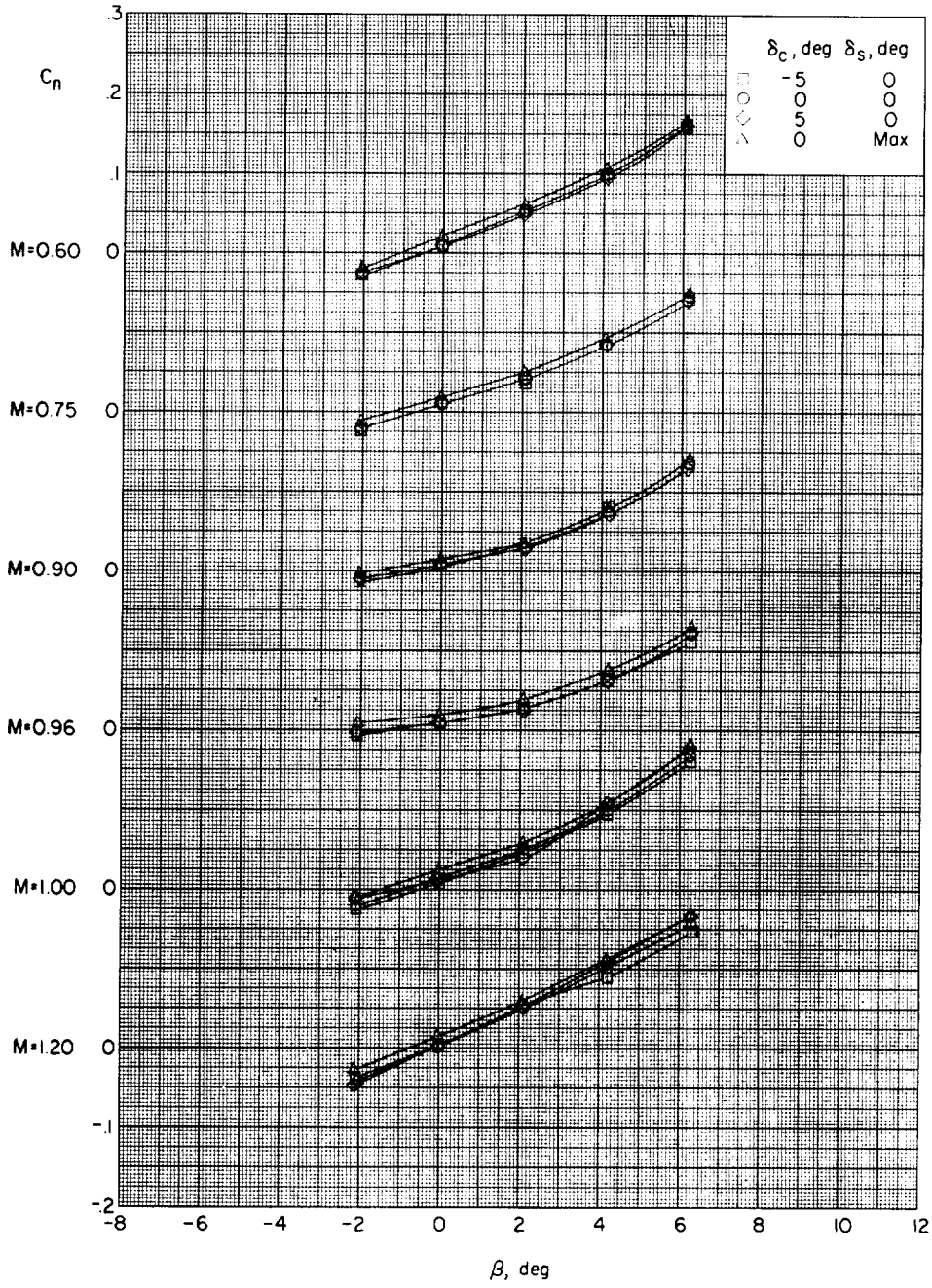

(a) Variation of C_n with β.

Figure 13.- Effect of control deflections on variation of C_n and C_l with β (drone with boosters). $\alpha \approx -6^\circ$.

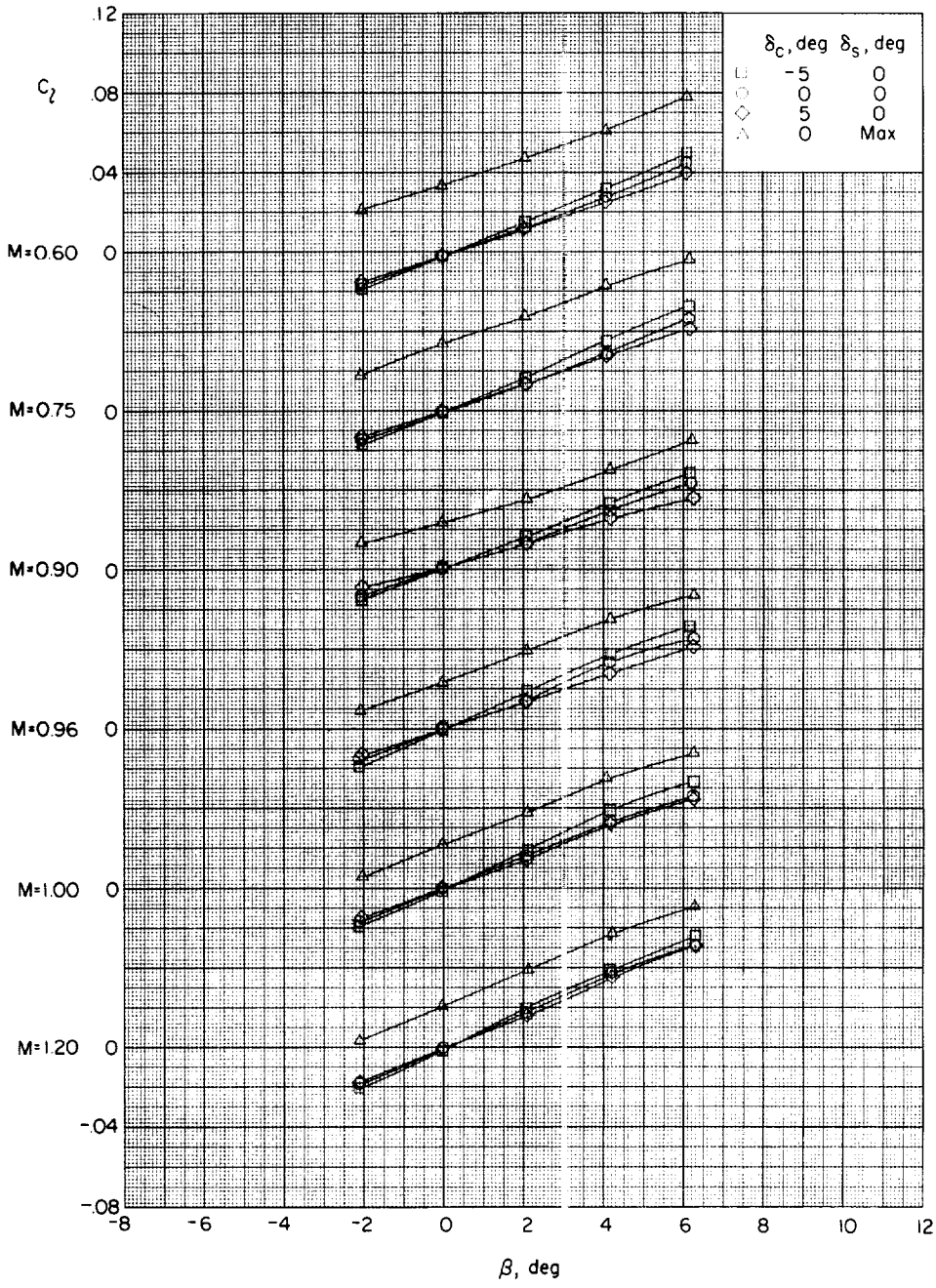

(b) Variation of C_l with β.

Figure 13.- Concluded.

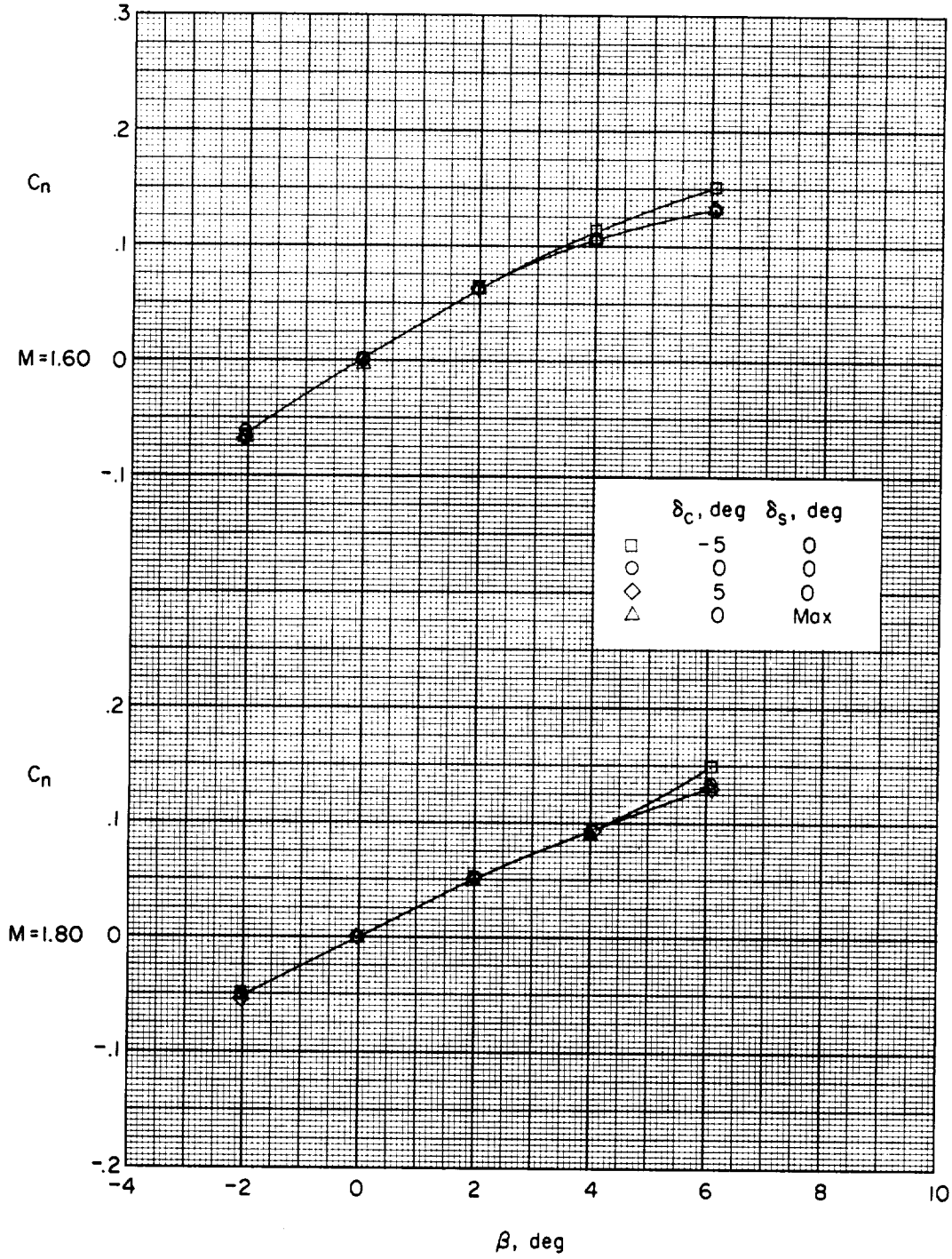

(a) Variation of C_n with β.

Figure 14.- Effect of control deflections on variation of C_n and C_l with β (drone with boosters). $\alpha \approx 5.2^\circ$.

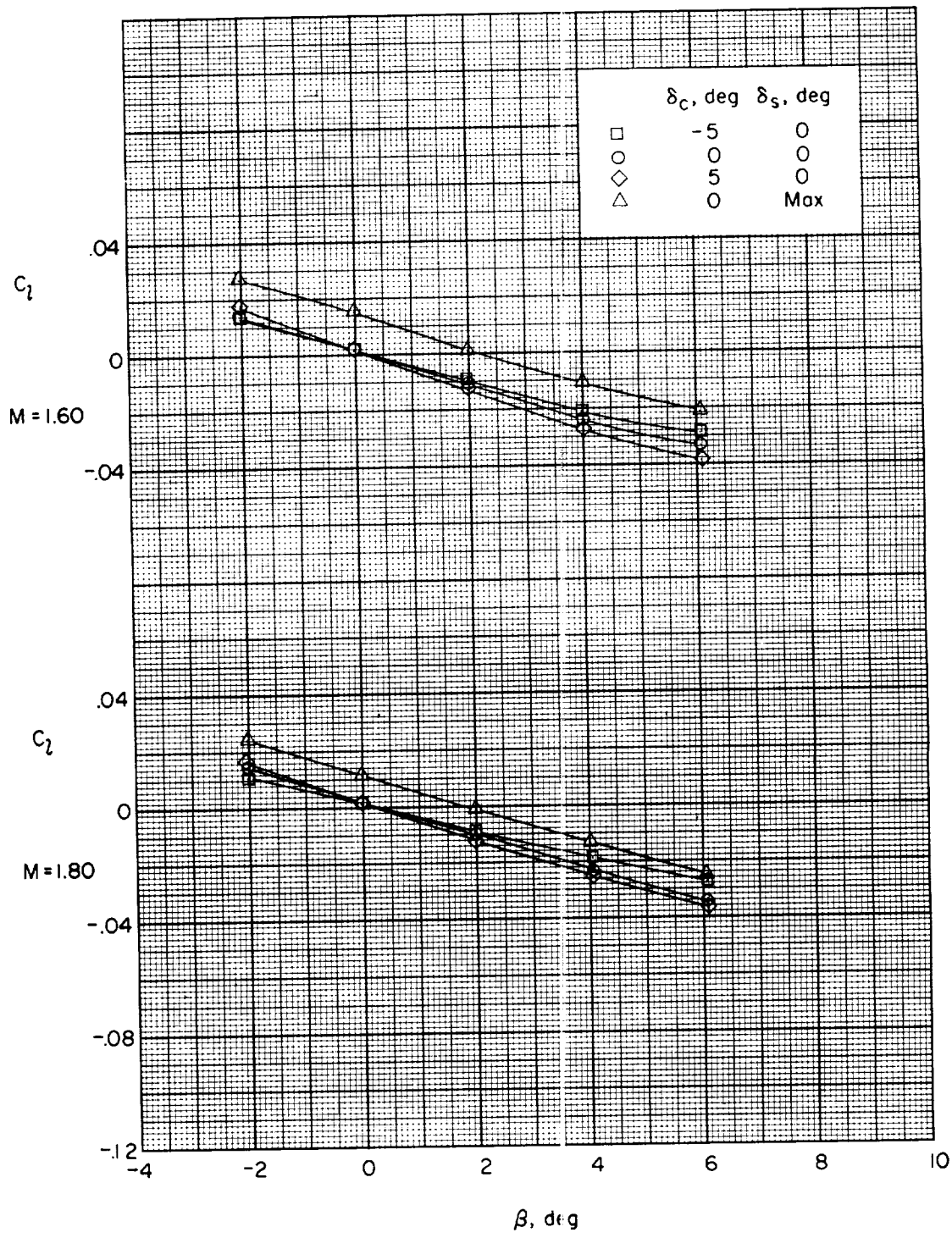

(b) Variation of C_l with β.

Figure 14.- Concluded.

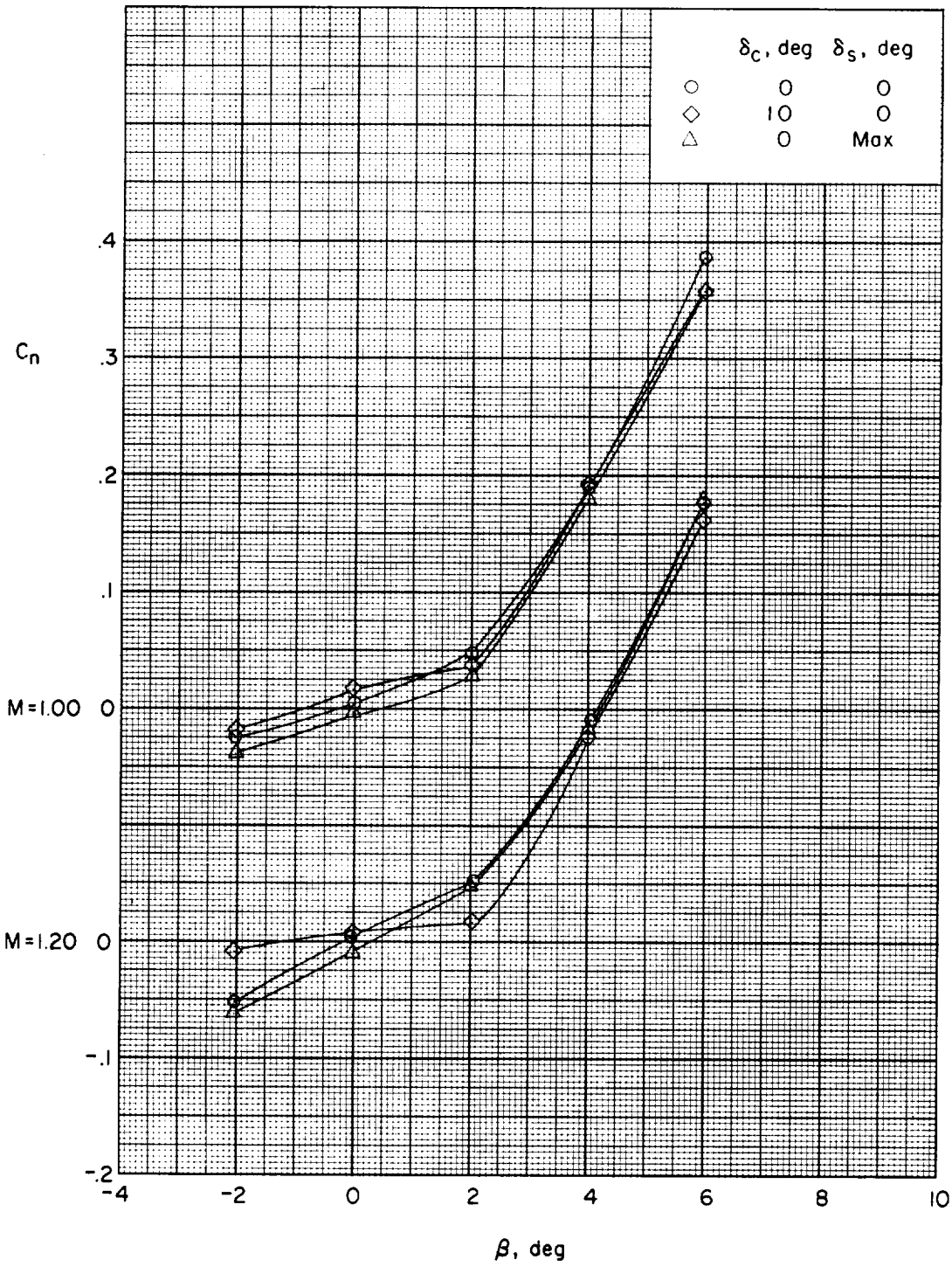

Figure 15.- Effect of control deflections on variation of C_n with β (drone without boosters). $\alpha \approx 11^\circ$.

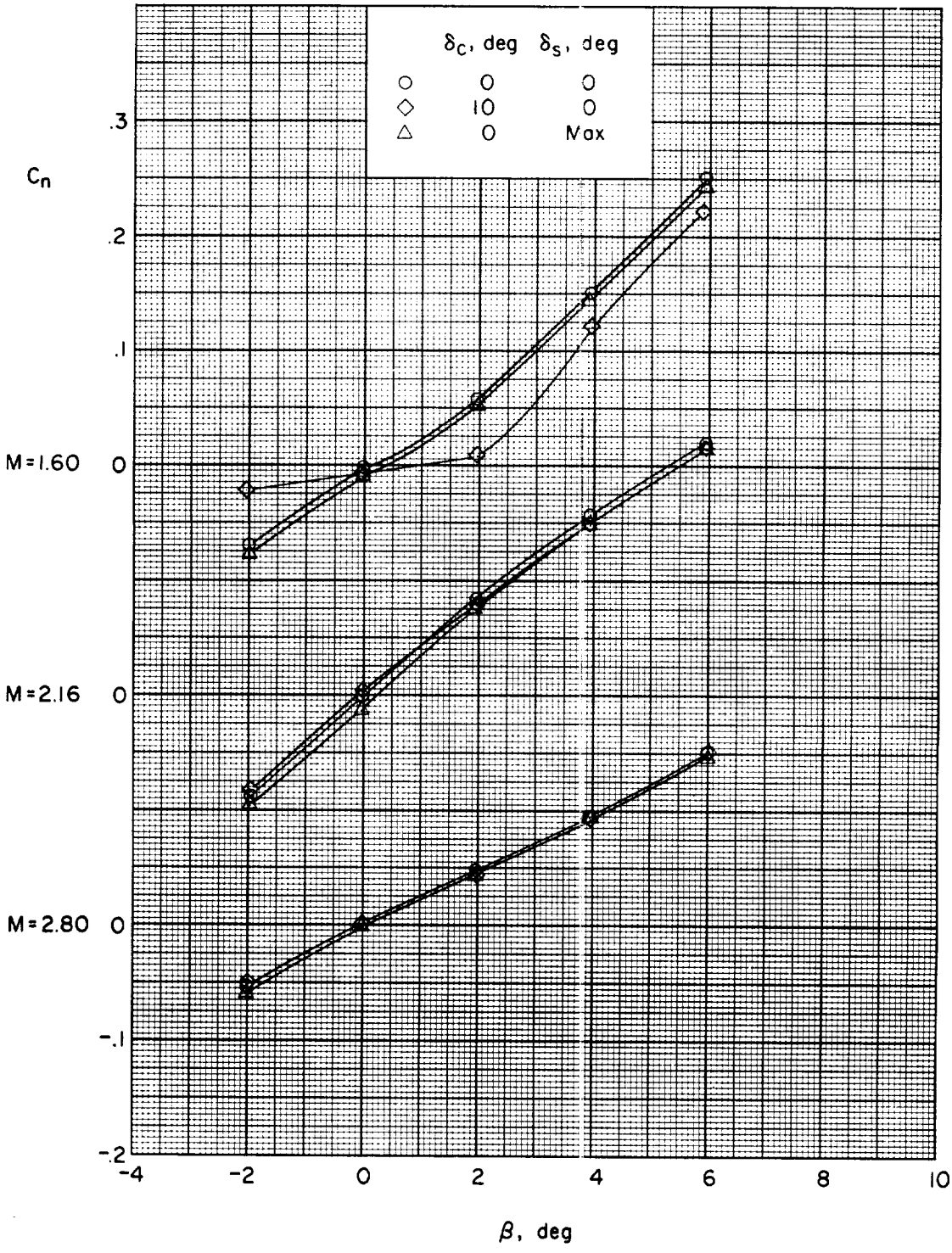

Figure 15.- Concluded.

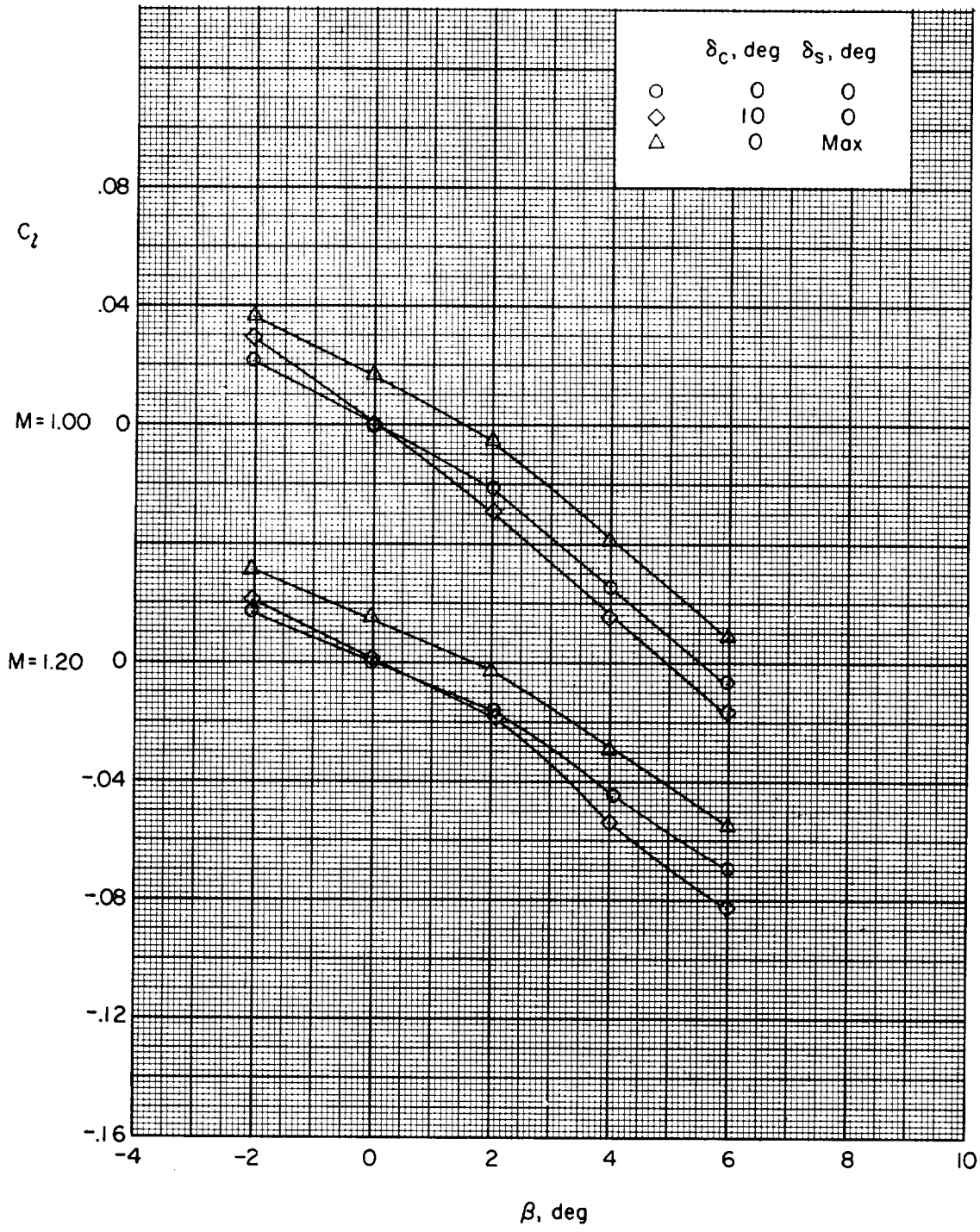

Figure 16.- Effect of control deflections on variation of C_l with β (drone without boosters). $\alpha \approx 11^\circ$.

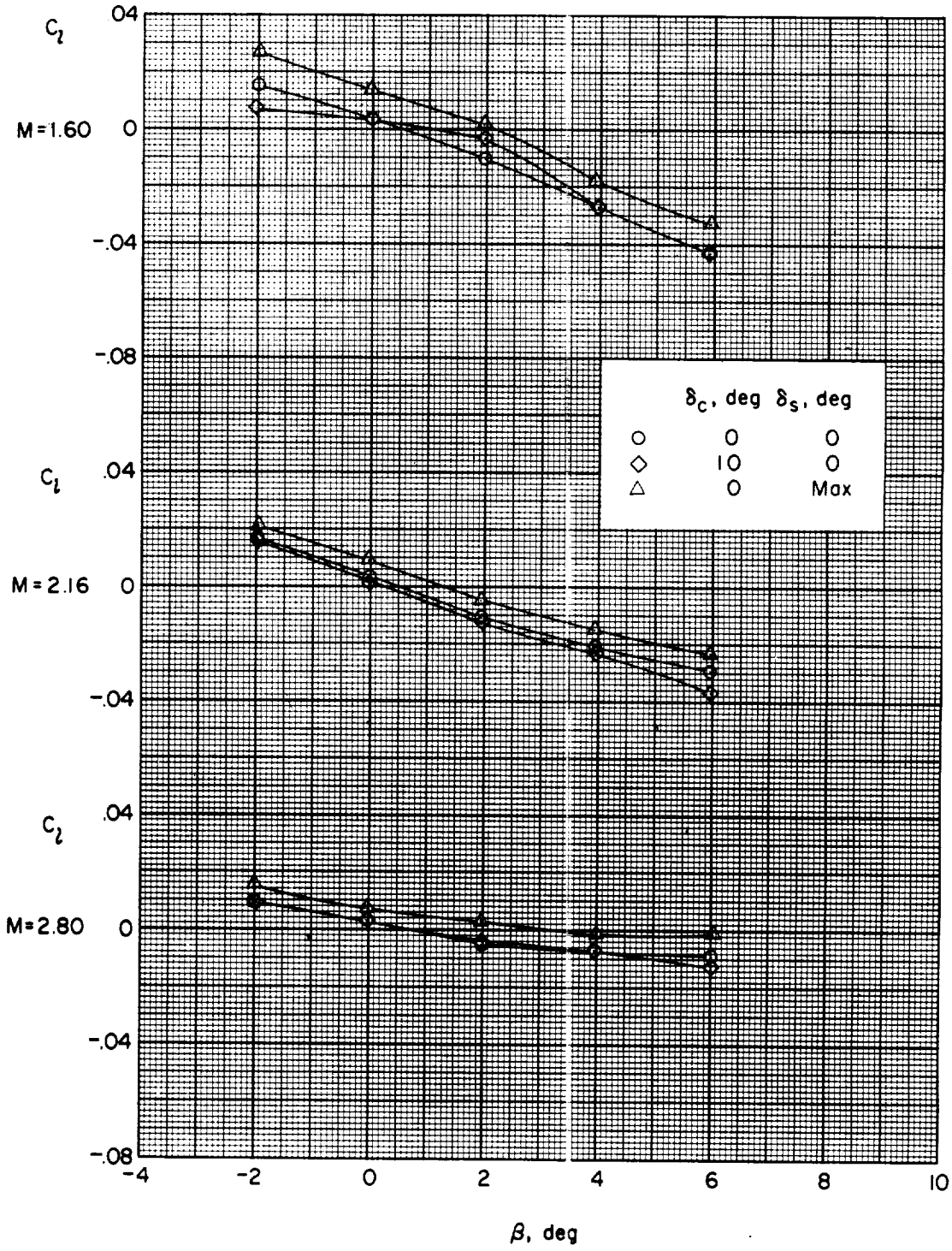

Figure 16.- Concluded.

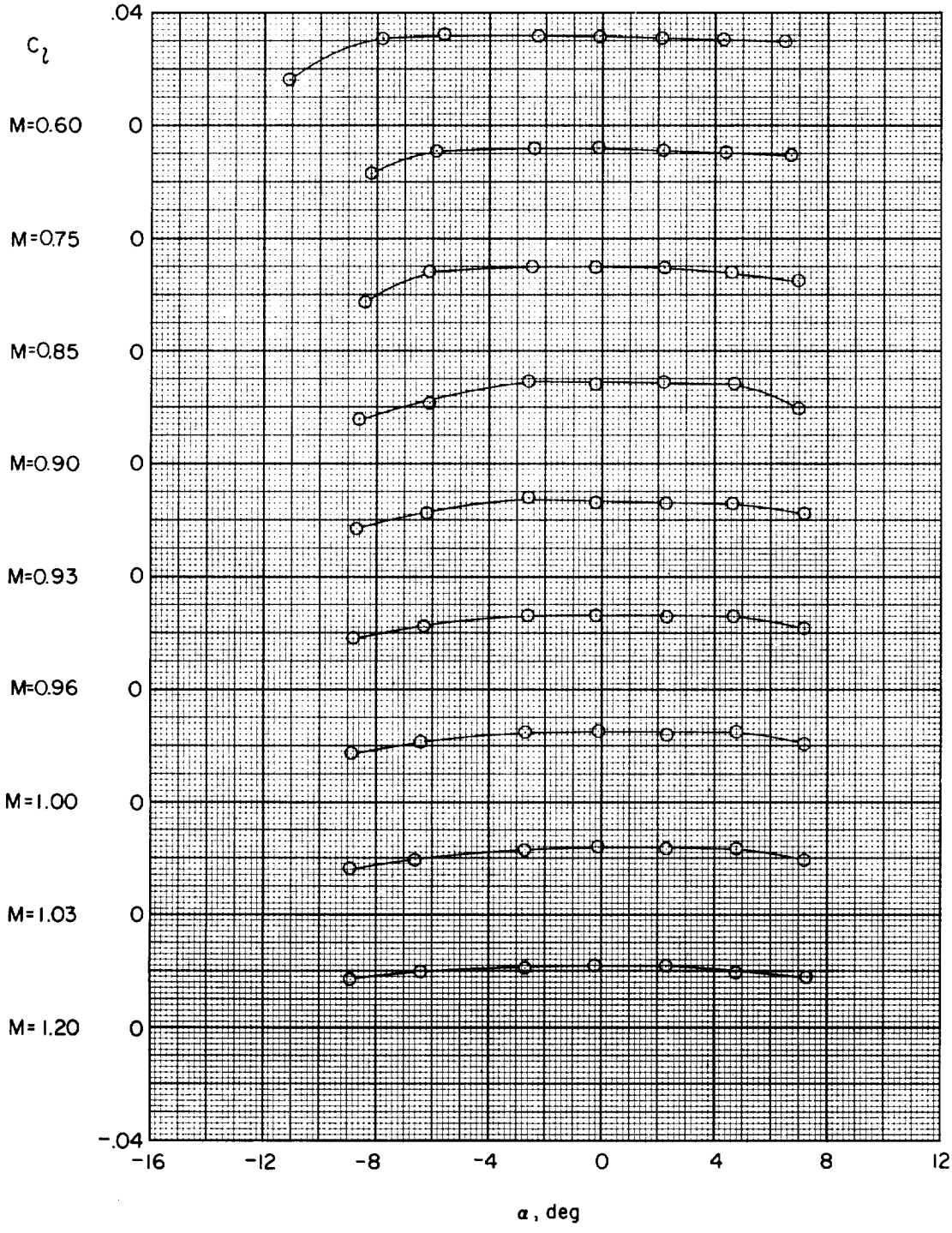

Figure 17.- Effect of maximum spoiler deflection on variation of C_l with α (drone with boosters). $\beta = 0^\circ$.

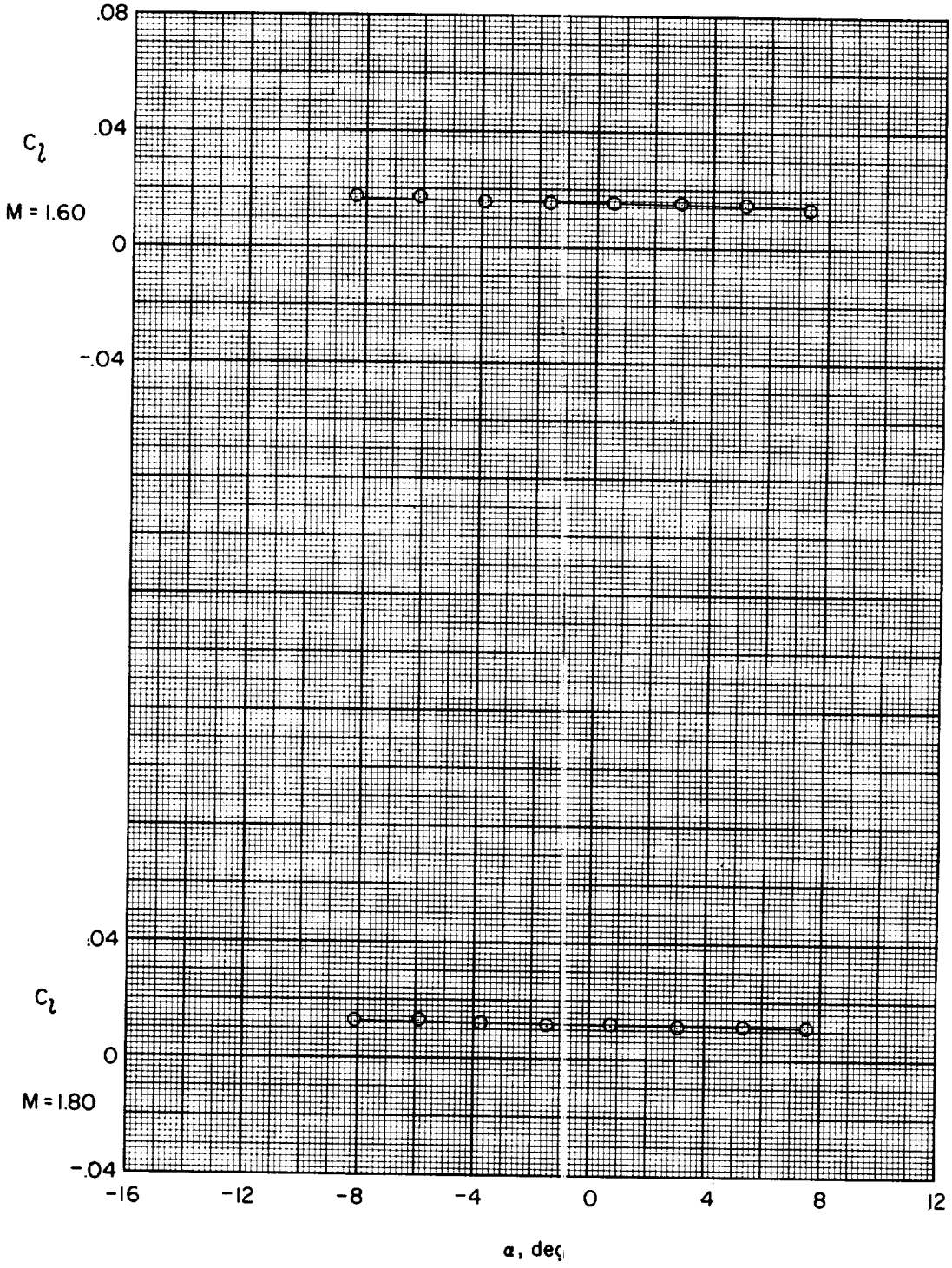

Figure 17.- Concluded.

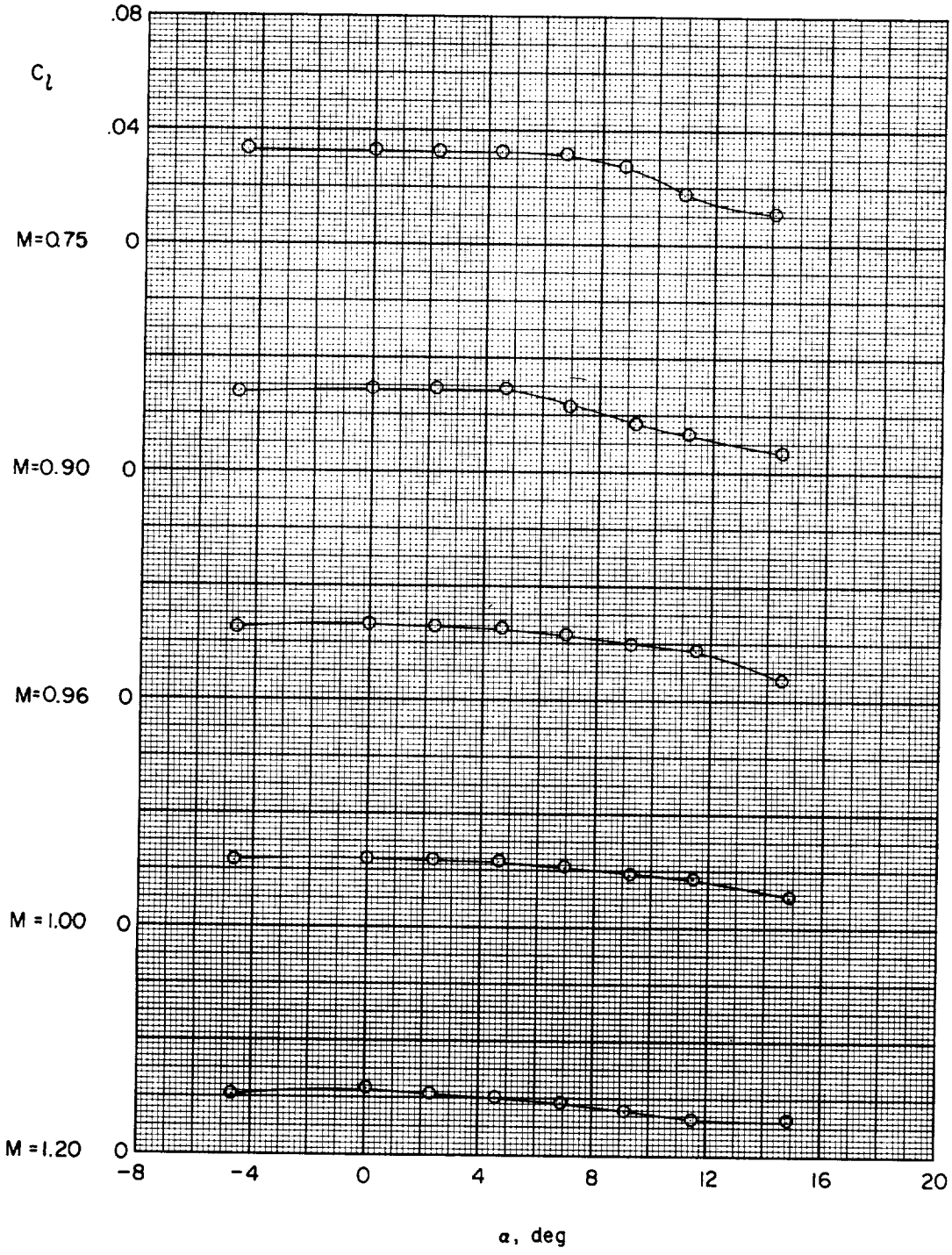

Figure 18.- Effect of maximum spoiler deflection on variation of C_l with α (drone without boosters). $\beta = 0^o$.

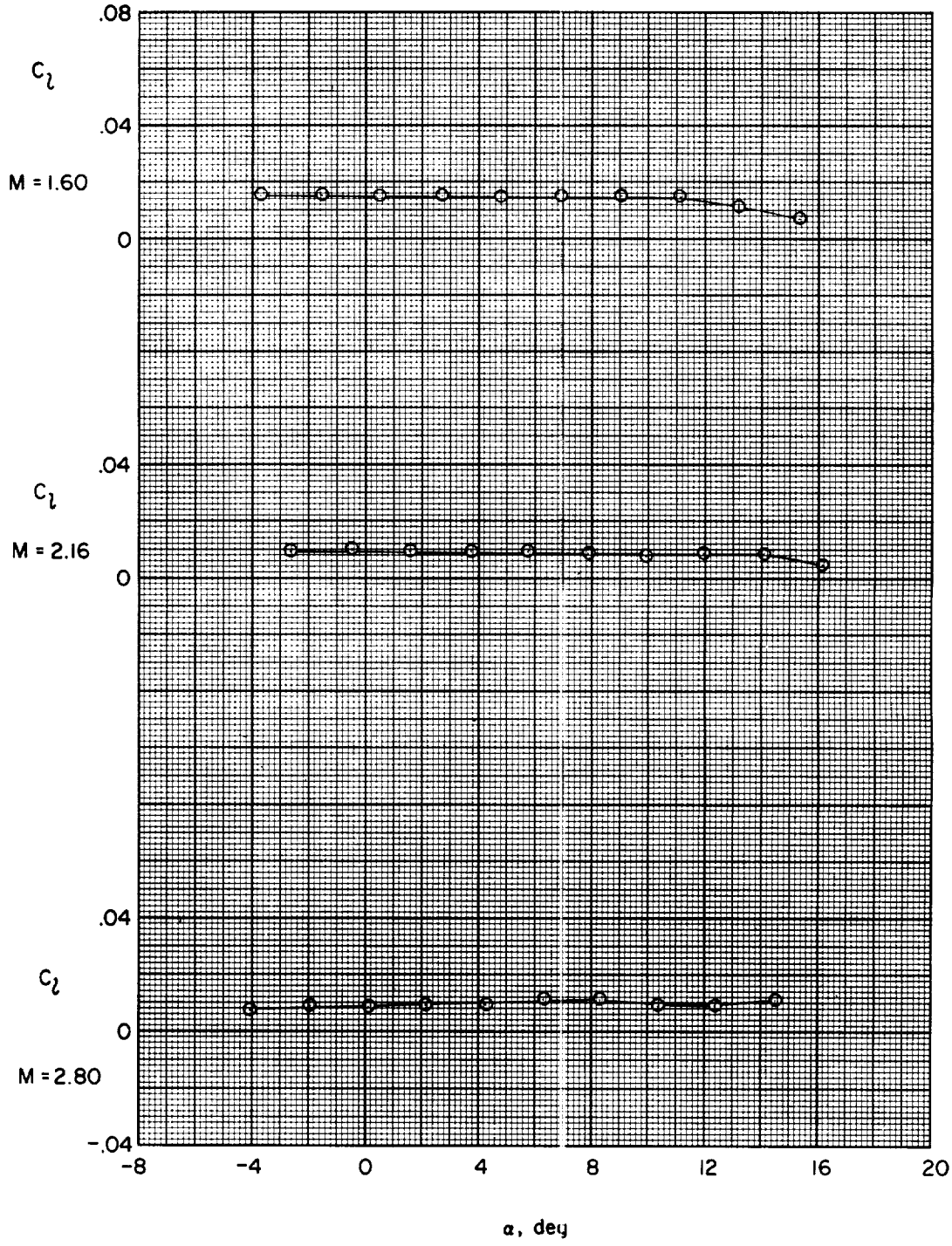

Figure 18.- Concluded.

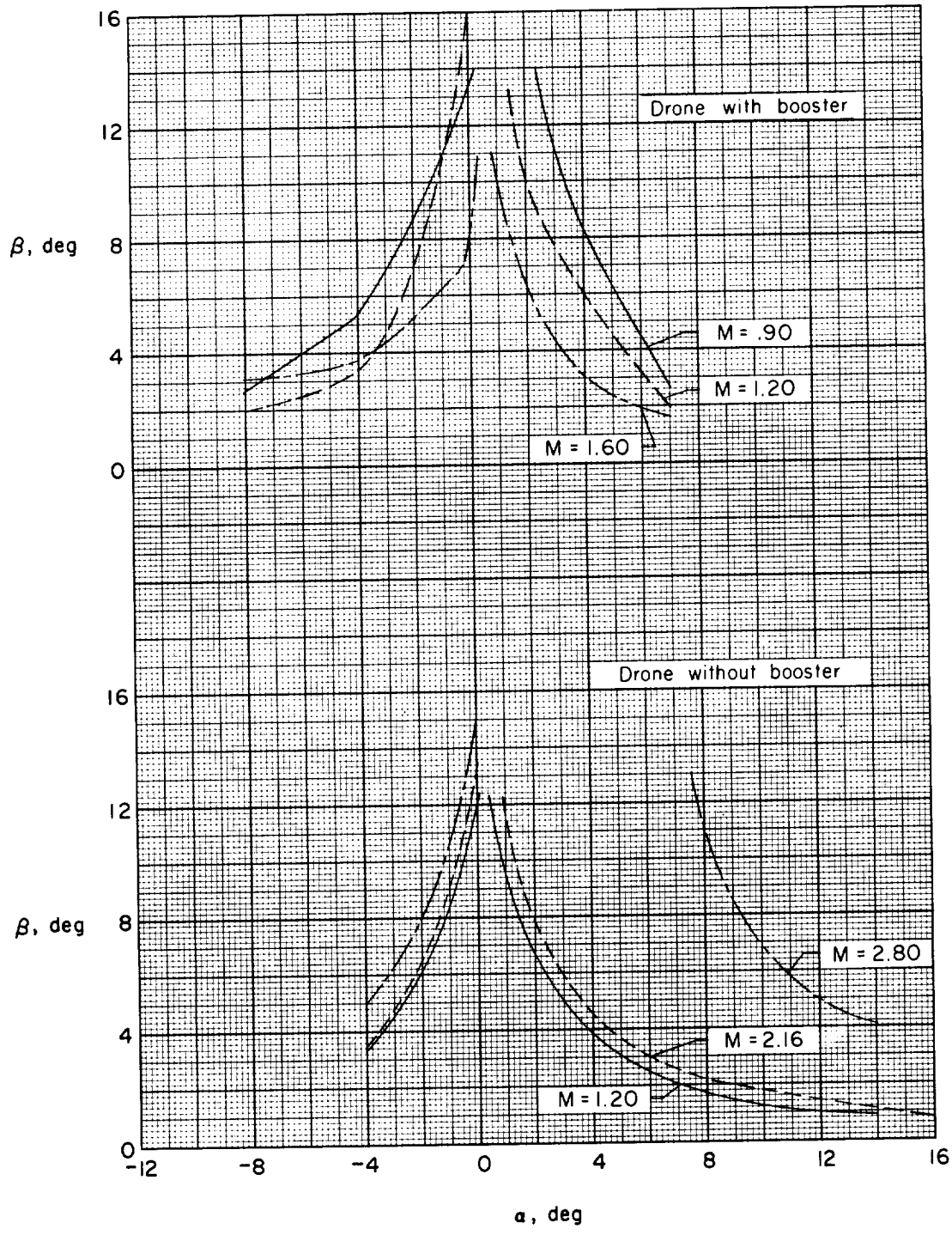

Figure 19.- Variation of trimmed angle of sideslip with angle of attack.